AJS American Journal of Science
publishing earth-sciences research since 1818

Encinas, A., Rosselot, E., Sagripanti, L., Folguera, A., Horton, B. K., Orts, D., Valencia, V. A., Arriagada, G., Butikofer, P., & Solórzano, A. (2024). Cenozoic Basin Evolution During Alternating Extension and Shortening in the Southern Central Andes Along the Chile-Argentina Border, 37–38°S. *American Journal of Science*, *324*, 5. https://doi.org/10.2475/001c.115328

Science Paper

Cenozoic Basin Evolution During Alternating Extension and Shortening in the Southern Central Andes Along the Chile-Argentina Border, 37–38°S

Alfonso Encinas[1a], Eduardo Rosselot[2], Lucía Sagripanti[2], Andrés Folguera[2], Brian K. Horton[3], Darío Orts[4,5], Victor A. Valencia[6], Gabriel Arriagada[1], Paz Butikofer[1], Andrés Solórzano[7]

[1] Departamento de Ciencias de la Tierra, Facultad de Ciencias Químicas, Universidad de Concepción, [2] Facultad de Ciencias Exactas y Naturales, Departamento de Ciencias Geológicas, Universidad de Buenos Aires, Instituto de Estudios Andinos "Don Pablo Groeber" (IDEAN), CONICET, Argentina, [3] Institute for Geophysics and Department of Earth and Planetary Sciences, Jackson School of Geosciences, the University of Texas at Austin, [4] Universidad Nacional de Río Negro, Instituto de Investigación en Paleobiología y Geología, [5] IIPG, UNRN, Consejo Nacional de Investigaciones científicas y Tecnológicas (CONICET), [6] School of the Environment, Washington State University, [7] Escuela de Geología, Departamento de Biología y Química, Facultad de Ciencias Básicas, Universidad Católica del Maule

Keywords: Andes, South-central Chile and Argentina, Principal Cordillera, Cura Mallín Formation, Trapa-Trapa Formation

https://doi.org/10.2475/001c.115328

American Journal of Science

Vol. 324, 2024

The south-central Chile and Argentina margin experienced a regional phase of extensional tectonics during the Oligocene–early Miocene, forming several basins across the forearc, Andean Cordillera, and retroarc regions. These basins accumulated thick successions of volcanic and sedimentary rocks. Subsequently, Neogene contractional tectonics led to the development of the current Andean Cordillera and the deposition of synorogenic clastic deposits in foreland basins. Traditionally, the Cura Mallín Formation, comprising a lower volcanic unit (CMV) and an upper sedimentary unit (CMS), has been interpreted to have formed during the Oligocene–early Miocene extensional phase. However, some studies propose deposition of the CMS in a foreland basin during the early–late Miocene. To unravel the transition from extensional to contractional tectonics in the Andes of south-central Chile and Argentina, we conducted new geochronological analyses (U-Pb, LA-ICP-MS) and integrated these results with structural, stratigraphic, and sedimentological observations in key sections within the CMS and the overlying Trapa-Trapa Formation in the Principal Cordillera along the Chile-Argentina border (37°–38°S). Our findings indicate that only the lower part of the CMS was deposited in an extensional setting, as evidenced by the presence of an inverted extensional wedge dated at ~20 Ma. The middle-upper CMS (~19 to 9 Ma) and contemporaneous units to the east exhibit evidence of syncontractional deformation, suggesting deposition in a foreland basin generated by shortening of the western Principal Cordillera. Around 9 Ma, uplift of the Agrio and Chos Malal fold and thrust belts, east of the Principal Cordillera, led to segmentation of the foreland basin. The Trapa Trapa Formation was deposited in a hinterland basin, with sediment sourced from the east. After ~6.5 Ma, major contractional deformation shifted westward, resulting in intense folding of the CMS and Trapa Trapa Formation and subsequent thrusting of the western Principal Cordillera over the Central Depression. Our study suggests that deformation progressed toward the eastern foreland during the early to late Miocene and then shifted toward the western forearc during the late Miocene to Pleistocene.

1. INTRODUCTION

The Chilean convergent margin is characterized by the subduction of an oceanic plate beneath South America, a process that has been ongoing probably since late Paleozoic times (Charrier et al., 2007; Oliveros et al., 2018). One of the most significant features of this margin is the Andean Cordillera, the longest and highest orogen formed in an ocean-continent convergent setting. This mountain range exhibits active contractional deformation due to the strong mechanical coupling between the oceanic and continental plates (Mpodozis & Ramos, 1990; Uyeda & Kanamori,

a Corresponding author: aencinas@udec.cl

1979). Other distinct features of the present Chilean margin include a volcanic arc situated within the Andes, a foreland basin to the east of this range, and a forearc to the west, typically characterized by a Coastal Cordillera and a Central Depression (Mpodozis & Ramos, 1990; Stern, 2002; Uyeda & Kanamori, 1979).

However, this configuration has not remained constant throughout the extensive geological history of the Chilean margin. The tectonic regime has frequently alternated between periods of shortening, extension, and quiescence (Charrier et al., 2007; Horton, 2018; Mpodozis & Ramos, 1990). These variations have led to changes in the characteristics of sedimentary basins, including their sedimentologic attributes and paleogeographic distributions along the margin (Charrier et al., 2007; Mpodozis & Ramos, 1990), as well as in volcanism, resulting in modifications to its location, volume, and magma composition (Charrier et al., 2007; Stern, 2002). The Chilean margin also exhibits significant along-strike segmentation, which is also reflected in the geological record. Some areas have experienced contractional deformation while others, during the same time periods, have undergone extension or remained in neutral tectonic conditions (e.g., Jordan et al., 2001; Oncken et al., 2006).

The causes of these variations in the tectonic regime over time and space have been a subject of extensive debate and have been linked to various mechanisms related to interactions between the oceanic and continental plates, including convergence rates (Somoza, 1998), the absolute westward motion of South America (Silver et al., 1998), the amount of sediment along the plate interface (Lamb & Davis, 2003), the age of the subducting plate (Yáñez & Cembrano, 2004), or the subduction of horizontal slab segments (Martinod et al., 2010), among others. While the exact mechanisms remain elusive, alternating tectonic regimes are common in many large orogenic belts, whether in oceanic subduction or continental collisional systems. Examples include the North American Cordillera, the European Alps, and the Himalayan-Tibetan orogenic systems (e.g., Kellett et al., 2019; Lister & Forster, 2009; Schlunegger & Kissling, 2015; Wells et al., 2012).

Among the most significant changes in the tectonostratigraphic evolution of the Chilean margin, one of the most notable occurred in south-central Chile and Argentina (33°–46°S) during the Oligocene–Miocene period. Throughout most of the early Cenozoic, this region underwent limited deposition, with relatively small basins accumulating modest thicknesses of sedimentary and volcanic deposits (Horton et al., 2016; Iannelli et al., 2018; Mpodozis & Ramos, 1990). However, during the late Oligocene to early Miocene, several forearc, intra-arc, and retroarc basins developed over an extensive area, spanning between the present Pacific and Atlantic coasts (fig. 1). These basins became filled with thick successions of volcanic, volcaniclastic, lacustrine, fluvial, and marine deposits (Jordan et al., 2001; Muñoz et al., 2000).

Volcanism and more restricted nonmarine sedimentation characterized this region initially (fig. 1; Elgueta et al., 2000; Encinas et al., 2018). Muñoz et al. (2000) observed that the early stages of this magmatic activity commenced in the Eocene in certain areas (e.g., Aragón et al., 2011; Charrier et al., 2002), with the most substantial volume of igneous rocks originating in the late Oligocene to early Miocene period. Successions several thousand meters thick primarily accumulated within intra-arc basins (Charrier et al., 2002; Jordan et al., 2001; Muñoz et al., 2000). Among these basins, the most renowned is that where the Abanico Formation accumulated (fig. 1), between approximately 33° and 36°S (Astaburuaga, 2014; Charrier et al., 1996, 2002). Limited volcanic activity also occurred in the forearc, forming what Muñoz et al. (2000) defined as the Coastal Magmatic Belt (fig. 1). Magmatic activity extended to the retroarc, resulting in extensive basalt plateaus, such as those of the Somuncura Formation located east of the Main Andean Cordillera and extending almost to the Atlantic coast (fig. 1; Kay & Copeland, 2006; Muñoz et al., 2000).

Following the deposition of volcanic rocks, a marine transgression, originating from both the Pacific and Atlantic, blanketed a substantial portion of southern South America, accumulating marine sediments with thicknesses of up to 1500 meters (fig. 1; Bechis et al., 2014; Elgueta et al., 2000; Encinas et al., 2012, 2018). Marine deposition commenced in the late Oligocene to early Miocene period (~26–23 Ma) and reached its maximum extent at approximately 20 Ma when, in some areas (41°–46°S), it nearly completely covered the forearc and retroarc domains and extended up to the present Andes (Encinas et al., 2018).

Several authors have linked the formation of upper Oligocene-lower Miocene basins to a regional episode of extensional tectonics (Charrier et al., 2002; Encinas et al., 2016, 2018; Jordan et al., 2001; Kay & Copeland, 2006; Muñoz et al., 2000). Evidence primarily relies on the geochemistry of volcanic rocks, which exhibit a complex mixture of slab signatures and pristine mantle sources, suggesting a thinned crust (Encinas et al., 2016; Fernández Paz et al., 2020; Jordan et al., 2001; Kay & Copeland, 2006; Muñoz et al., 2000). In addition, structural studies conducted on outcrops and seismic lines reveal the presence of synextensional sedimentation in volcanic and sedimentary deposits (Elgueta et al., 2000; Encinas et al., 2016; Fennell et al., 2019; García Morabito & Ramos, 2012; Melnick & Echtler, 2006; Orts et al., 2012).

Notably, certain areas in the eastern forearc and the Andes (~41°–46°S) feature upper Oligocene-lower Miocene marine deposits interbedded with volcanic lavas from the Traiguén and Ventana formations (fig. 1; Encinas et al., 2016; Fernández Paz et al., 2020). Additionally, Encinas et al. (2014) reported the presence of both Pacific and Atlantic molluscan taxa in upper Oligocene–lower Miocene marine strata in the Andes at ~43°S, suggesting a temporary connection between both seas during this period. These findings imply that the Andean Cordillera, at least at the mentioned latitudes, had likely not yet formed. The presence of uplifted upper Oligocene–lower Miocene marine strata reaching elevations of approximately 2000 m above sea level indicate that Andean shortening took place after the early Miocene (Bechis et al., 2014; Encinas et al., 2019; Fernández Paz et al., 2020). Nevertheless, Colwyn

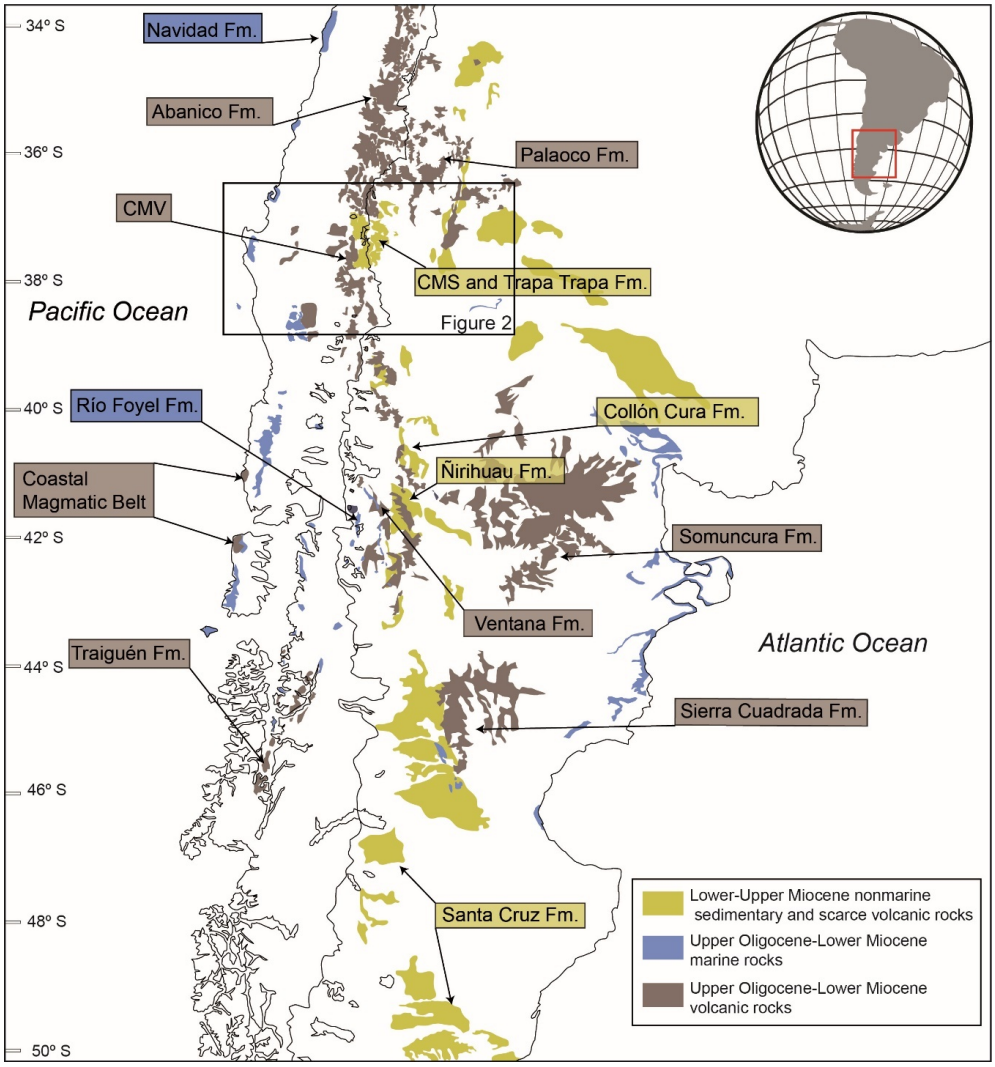

Figure 1. Oligocene–Miocene sedimentary and volcanic deposits in southern South America (~34°–50°S).

The figure includes labels indicating the names of the most significant units.

et al. (2019) proposed that the North Patagonian Andes between 46° and 51°S experienced Cretaceous growth, remaining elevated during the Cenozoic, based on the analysis of water isotopes extracted from hydrated volcanic glass. However, the presence of upper Oligocene–lower Miocene marine strata of the Guadal Formation along the current Andean axis at 46°–47° (Encinas et al., 2019), as well as coeval deep marine strata of the Traiguén Formation in the eastern part of the forearc at approximately the same latitudes (Encinas et al., 2016), suggests that if such uplift did occur, it likely formed a relatively narrow area.

The causes of extension and widespread volcanism during this period have been attributed to a plate reorganization in the southeast Pacific, resulting in a transition from slower, more oblique South America-Farallón convergence to a more rapid, near-normal South America-Nazca convergence at approximately 26–28 Ma (Jordan et al., 2001; Kay & Copeland, 2006; Muñoz et al., 2000). Muñoz et al. (2000) proposed that this change in subduction geometry induced a transient phase of vigorous asthenospheric-wedge circulation, accelerating slab rollback, which, in turn, led to regional extension and widespread volcanism.

After the sedimentation of volcanic or marine rocks during the late Oligocene-early Miocene extensional phase, the region located between 33° and 46°S witnessed the deposition of extensive successions of lower-upper Miocene fluvial, alluvial, and lacustrine clastic deposits (fig. 1; Cuitiño et al., 2016; Encinas et al., 2018; Giambiagi et al., 2016; Horton & Fuentes, 2016; Orts et al., 2012; Rojas Vera et al., 2015. While the deposits from the earlier phase covered most of the margin, including forearc, intra-arc, and retroarc basins, the younger nonmarine Miocene deposits are confined to the eastern part of the Andes and the foreland (fig. 1). Lower-upper Miocene clastic deposits have typically been interpreted as having been deposited in foreland basins. This interpretation is based on the presence of syncontractional growth strata, an increase in grain size and thickness toward the hinterland, and provenance analysis suggesting source areas located in the western part of the Andes (Folguera et al., 2018; Giambiagi et al., 2003; Giambiagi & Ramos, 2002; Horton et al., 2016; M. E. Ramos et al., 2011). It has been proposed that the growth of the Andes and the deposition of synorogenic Miocene deposits occurred subsequent to the inversion of prior Oligocene-

lower Miocene extensional basins, such as the Abanico basin. The progressive advance of deformation toward the east led to the incorporation of part of the Miocene synorogenic deposits into the Andean region (Astini & Dávila, 2010; Farías et al., 2010; Fock, 2005; Fock et al., 2006; Giambiagi et al., 2003).

With very few exceptions (e.g., Mosolf et al., 2018), there is a strong consensus that the Oligocene-lower Miocene volcanic and sedimentary rocks mentioned above were deposited within an extensional tectonic framework (Elgueta et al., 2000; Encinas et al., 2016, 2018; Fennell et al., 2019; García Morabito & Ramos, 2012; Jordan et al., 2001; Melnick & Echtler, 2006; Muñoz et al., 2000; Orts et al., 2012). Conversely, some authors differ from the interpretation of a contractional tectonic setting for some of the Miocene sedimentary units that crop out in the Andean Cordillera (fig. 1; Jordan et al., 2001; Spalletti & Dalla Salda, 1996; Suárez & Emparán, 1995). One notable case pertains to the Cura Mallín Formation. This unit was initially defined in the Laguna del Laja area (Principal Cordillera, Chile, ~37°–38°S; figs. 1, 2, and 3) as a sedimentary formation with some volcanic intercalations by O. González and Vergara (1962). Subsequently, Niemeyer and Muñoz (1983) subdivided this unit into a lower volcanic member (CMV from now on) and an upper sedimentary member (CMS from now on). Muñoz and Niemeyer (1984) and Suárez and Emparán (1995) expanded the boundaries of this unit to encompass Oligocene-Miocene volcanic and sedimentary rocks previously attributed to other formations across a wide area of the Principal Cordillera spanning from 36° to 38°S (figs. 2 and 3).

The stratigraphy, age, and tectonic context of the Cura Mallín Formation have been extensively debated due to various factors. These include the absence of continuous sections, the intricate nature of a unit that spans a considerable area and encompasses diverse lithologies, the inconsistencies of published ages, and the limited availability of structural data. In terms of the tectonic setting of this unit, Suárez and Emparán (1995) and Spalletti and Dalla Salda (1996) initially proposed that the Cura Mallín Formation, including the CMV and CMS, was deposited in pull-apart basins formed by transtensional tectonics. However, they did not offer clear structural evidence to support this claim. Subsequently, Jordan et al. (2001) suggested that the Cura Mallín Formation was accumulated in an intra-arc extensional basin, based on their interpretation of synextensional strata in a seismic line from the Río Lileo area (Principal Cordillera, Argentina, ~37°S). Jordan et al. (2001) also posited that the volcanic (CMV) and sedimentary (CMS) rocks within the Cura Mallín Formation are interdigitated, based on similar late Oligocene–early Miocene Ar/Ar ages for both units (figs. 3, 4, and 5, and table 1). Drawing on these ages and structural evidence, Jordan et al. (2001) concluded that the CMV and CMS units are both contemporaneous with the Abanico Formation and other volcanic and sedimentary units deposited in an extensional setting along the South American margin between 33° and 45°S (fig. 1). This perspective gained widespread acceptance among the majority of researchers (e.g., Folguera et al., 2010; Kay & Copeland, 2006; Radic et al., 2002; Rojas Vera et al., 2016; Zapata & Folguera, 2005).

Nonetheless, several datasets raise questions about this framework. The supposed interdigitation between the CMV and the CMS is solely based on two radiometric ages but has never been observed (Jordan et al., 2001). Flynn et al. (2008) reported younger early–middle Miocene ages for the CMS in the Laguna del Laja area (situated to the west of the Río Lileo area studied by Jordan et al., 2001; figs. 2, and 3), while Suárez and Emparán (1995) obtained early–late Miocene ages for the CMS and the CMV in the Lonquimay area (38°–39°S; figs. 2, 3, 4, and 5, and table 1). In relation to the tectonic setting, Cobbold and Rossello (2003) and Cobbold et al. (2008) challenged the interpretation of Jordan et al. (2001) and instead suggested that the sedimentary rocks of the CMS were deposited in a foreland basin. This interpretation is based on the presence of syncontractional growth strata within this unit in the Río Lileo area.

Another challenging aspect relates to determining the timing of the initiation of contractional tectonics and the onset of Andean growth in the region. In the Eastern Principal Cordillera, the CMS is overlain by sedimentary and volcanic rocks of the Trapa Trapa Formation. The age of this formation is also discussed (fig. 4). Jordan et al. (2001) assigned it to the late early Miocene, while Flynn et al. (2008) proposed a late Miocene age. The strata within the CMS and Trapa Trapa formations exhibit significant deformation, indicating that contractional tectonics commenced either during or after the deposition of these units. Jordan et al. (2001), in their analysis of seismic data from the Río Lileo area, suggested that tectonic inversion in the region began during or after the deposition of the Trapa Trapa Formation, as they identified potential synorogenic strata within this unit. Lower to middle Miocene nonmarine clastic deposits are also present in the Agrio and Chos Malal Fold and Thrust Belts (FTBs) to the east, and these have been interpreted as products of contractional tectonics, based on the presence of syncontractional features (e.g., V. A. Ramos, 1998; Zamora Valcarce et al., 2006). Due to the disparity in reported ages for the CMS and Trapa Trapa formations (figs. 4, and 5, and table 1), the correlation of these units with the Miocene deposits of the FTBs remains uncertain. Consequently, deciphering the tectonic evolution of the Andean Cordillera in this area, encompassing both the Principal Cordillera and the FTBs, during the Neogene has proven elusive. This uncertainty also hinders comparisons of the tectonic evolution of this region with other areas in the Andes of south-central Chile and Argentina.

Our primary research objective is to gain insight into a pivotal event in the geological evolution of the Andes in south-central Chile and Argentina during the middle to late Cenozoic period: the transition from extensional to contractional tectonics that ultimately shaped the contemporary Andean Cordillera. The findings of this study hold the potential to shed light on analogous scenarios in other orogenic belts that have experienced alternating tectonic regimes (e.g., Kellett et al., 2019; Lister & Forster, 2009; Schlunegger & Kissling, 2015; Wells et al., 2012). Our in-

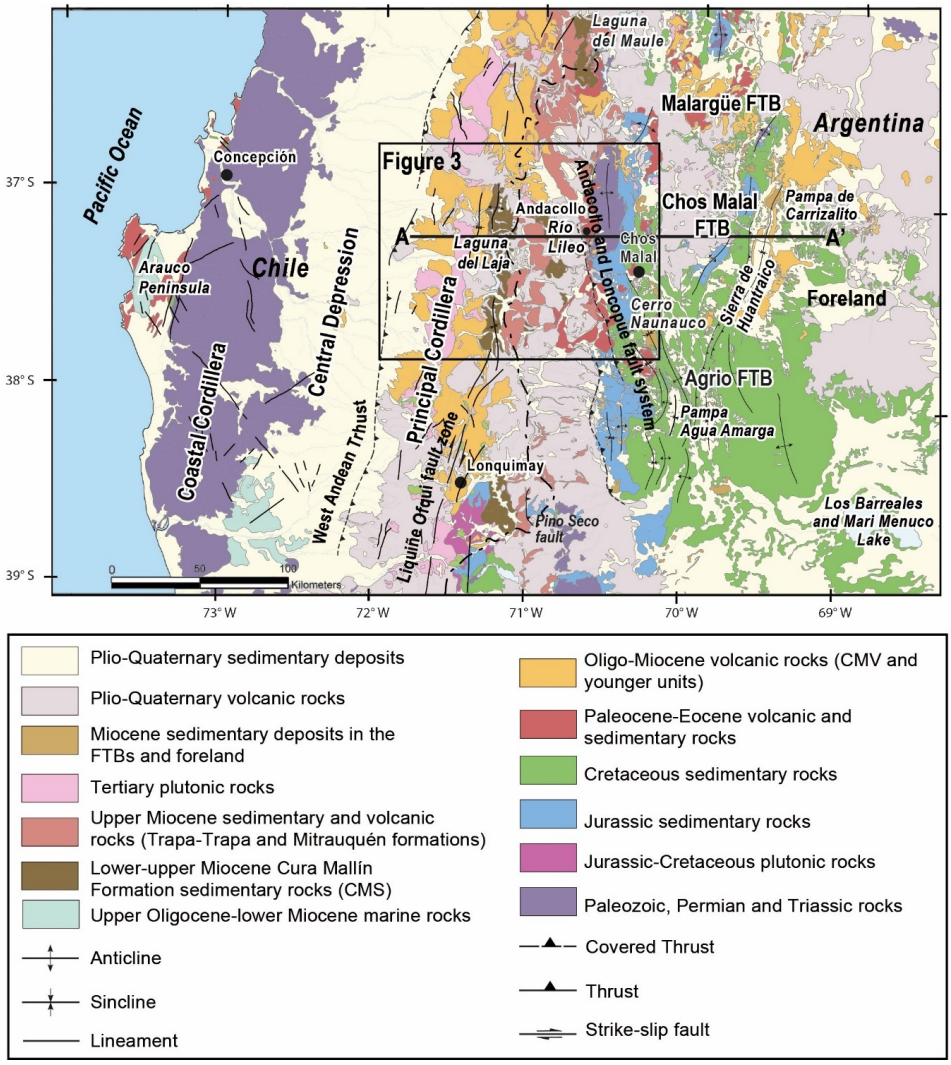

Figure 2. Regional geological map of south-central Chile and Argentina (~36°–39°S).

The Cura Mallín Formation, including the volcanic (CMV) and sedimentary (CMS) rocks traditionally assigned to this unit, crop out in the Laguna del Maule, Laguna del Laja-Río Lileo, and Lonquimay areas. The inset shows the location of figure 3. Line A–A' indicates the position of the topographic profile presented in figure 5. The figure is adapted from Sernageomin (2003); Zamora Valcarce (2007), Melnick et al. (2006), Rojas Vera et al. (2016); Sagripanti et al. (2016).

vestigation revolves around several fundamental questions: Does the tectonic evolution of the Cura Mallín basin differ from that of neighboring regions in the Andes to the north and south? Was the Cura Mallín Formation deposited within an intra-arc extensional basin comprising contemporaneous volcanic (CMV) and sedimentary (CMS) rocks, as proposed by Jordan et al. (2001)? Alternatively, do the CMS deposits represent synorogenic strata resulting from Andean mountain-building? What is the age of the CMS, and how does it correlate with other geological units in the surrounding region and the broader Andes of south-central Chile and Argentina? Are the divergent age assignments (late Oligocene–early Miocene vs. early–middle Miocene) proposed by different authors (e.g., Flynn et al., 2008; Jordan et al., 2001; Suárez & Emparán, 1995) accurate, and can any disparities be attributed to diachronic sedimentation as proposed by Radic et al. (2002)? Or are some of these age assignments potentially erroneous, as suggested by Flynn et al. (2008)?

In our quest to address these inquiries, we conducted new geochronological analyses (U-Pb, LA-ICP-MS) complemented by structural, stratigraphic, and sedimentological observations in key sections within the Cura Mallín Formation and the overlying Trapa-Trapa Formation in the Laguna del Laja-Río Lileo regions (37°–38°S). By integrating our findings with previous research conducted in the region, particularly studies carried out in the Malargüe and Chos Malal Fold and Thrust Belts (FTBs) to the east, we shed new light on the tectonic evolution of the Andes at these latitudes. This integration has enabled us to establish correlations between the Miocene deposits within this geographical domain, specifically the CMS and Trapa-Trapa formations, and similar units in the Agrio and Chos Malal FTBs located to the east. Furthermore, we have achieved the capacity to correlate these findings with corresponding units within the Andes, both to the north and south of our study area.

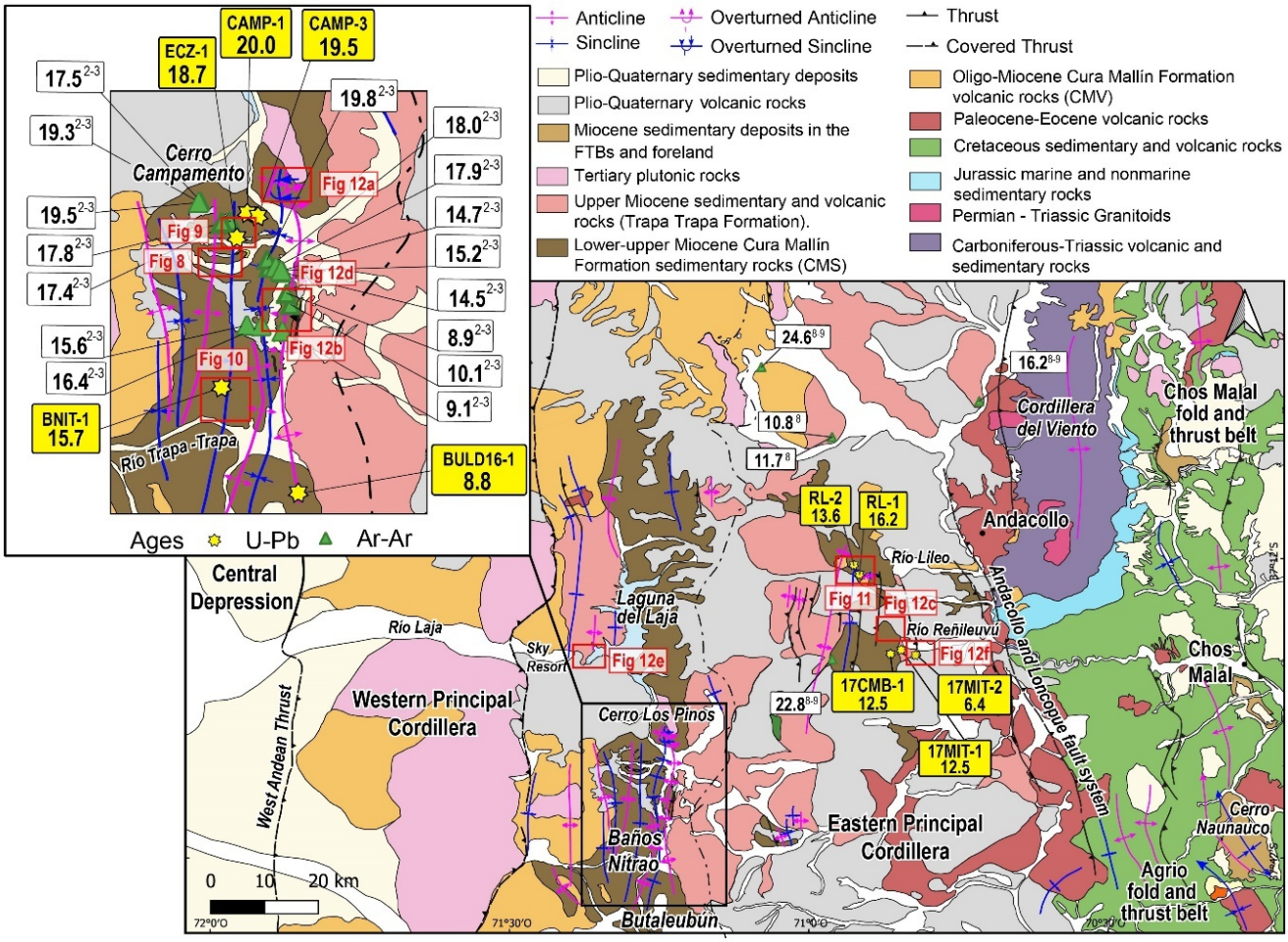

Figure 3. Geologic map of the Laguna del Laja-Río Lileo study area showing geologic units, primary tectonic structures, and radiometric ages from previous authors (Ar/Ar) and the present study (U-Pb).

Ar/Ar ages, represented by green triangles and white rectangles, are from Herriott (2006)[2], Flynn et al. (2008)[3], Burns et al. (2006)[8], and Jordan et al. (2001)[9]. The corresponding numbers can be cross-referenced with those in table 1. U-Pb ages, denoted by yellow stars and yellow rectangles, are derived from the current study (see figures 6 and 7, and table S1 for more details). The geologic map is adapted from Niemeyer and Muñoz (1983), Melnick et al. (2006), and Rojas Vera et al. (2016).

2. GEOLOGIC SETTING

To achieve a comprehensive understanding of the regional geological context pertinent to the Oligocene–Miocene units under investigation in this study, specifically the Cura Mallín and Trapa Trapa formations, the first subsection of this chapter delineates the most significant geological characteristics in the area where these units are exposed (fig. 2; 36°–39°S). This encompasses the primary morphostructural units, notable structural features, and the distribution of Paleozoic, Mesozoic, and Cenozoic rocks. The latter aspect is particularly important for comprehending the potential source areas for the CMS and Trapa Trapa formations, which will be discussed in subsequent chapters. The second subsection explores previous studies conducted on the Cura Mallin and Trapa Trapa formations, as well as on the Oligocene-Miocene units in the eastern Agrio and Chos Malal FTBs. The objective is to clarify the stratigraphic and geochronological aspects addressed in our study.

2.1. REGIONAL GEOLOGIC CHARACTERISTICS

The southern-central Chile and Argentina margin, spanning approximately 36° to 39°S, exhibits the following morphostructural units from west to east: the Coastal Cordillera, Central Depression, Principal Cordillera, Agrio and Chos Malal Fold and Thrust Belts, and the foreland (figs. 2, and 3).

The Coastal Cordillera (fig. 2) is a low-profile mountain range, with maximum elevations reaching around ~1500 m (Encinas et al., 2021). It primarily consists of upper Paleozoic-Triassic metamorphic rocks and Carboniferous-Permian plutonic rocks (Sernageomin, 2003). In certain coastal areas, upper Cretaceous, Paleocene-Eocene, and Oligocene to Pleistocene volcanic, marine, and non-marine sedimentary rocks are exposed (García, 1968; Sernageomin, 2003; Stinnesbeck, 1986). The Coastal Cordillera is a relatively young morphostructural feature that uplifted in the past 2 Myr (Encinas et al., 2021).

The Central Depression (fig. 2) is a region of low relief situated between the Coastal Cordillera and the Principal Cordillera, with elevations typically ranging from 100 to

Table 1. Compilation of published ages for the Oligocene-Miocene units that crop out in the Principal Cordillera, the Agrio and Chos Malal Fold and Thrust Belts, and the foreland between ~37° and 39°S.

LOCALITY	UNIT	LITHOLOGY	METHOD	AGE (Ma)	LOCATION	REFERENCE
Principal Cordillera						
Laguna del Laja						
	CMV? TT?	Lithic tuff	K/Ar	13.7±1.4 (1σ)	Not indicated	1
	CMV? TT?	Lithic tuff	K/Ar	14.8±0.7 (1σ)	Not indicated	1
	CMV? TT?	Andesite	K/Ar	15.6±0.5 (1σ)	Not indicated	1
	CMV? TT?	Andesite	K/Ar	18.4±0.8 (1σ)	Not indicated	1
	TT	Basaltic andesite	Ar/Ar	8.90±0.1 (2σ)	37.61083°S, 71.21935°W	2; 3
	TT	Basaltic andesite	Ar/Ar	9.10±0.1 (2σ)	37.64236°S, 71.21979°W	2; 3
	TT	Basaltic andesite	Ar/Ar	10.10±0.2 (2σ)	37.61958°S, 71.21530°W	2; 3
	TT		Mammals	middle-late Miocene	~37.60696°S, ~71.22436°W	2; 3
	CMS	Ignimbrite	Ar/Ar	14.50±0.5 (2σ)	37.59237°S, 71.22329°W	2; 3
	CMS	Ignimbrite	Ar/Ar	14.70±0.6 (2σ)	37.59101°S, 71.22385°W	2; 3
	CMS	Tuff	Ar/Ar	15.20±0.2 (2σ)	37.59098°S, 71.22424°W	2; 3
	CMS	Ignimbrite	Ar/Ar	15.60±0.1 (2σ)	37.63839°S, 71.25048°W	2; 3
	CMS	Ignimbrite	Ar/Ar	16.40±0.3 (2σ)	37.63852°S, 71.23809°W	2; 3
	CMS	Tuff	Ar/Ar	17.40±0.5 (2σ)	37.55256°S, 71.27297°W	2; 3
	CMS	Tuff	Ar/Ar	17.70±0.2 (2σ)	37.55144°S, 71.27243°W	2; 3
	CMS	Ignimbrite	Ar/Ar	17.84±0.2 (2σ)	37.54999°S, 71.26592°W	2; 3
	CMS	Ignimbrite	Ar/Ar	17.90±0.4 (2σ)	37,58890°S, 71.22857°W	2; 3
	CMS	Ignimbrite	Ar/Ar	18.00±0.3 (2σ)	37.58816°S,	2; 3

LOCALITY	UNIT	LITHOLOGY	METHOD	AGE (Ma)	LOCATION	REFERENCE
					71.23398°W	
	CMS	Tuff	Ar/Ar	17.5±0.4 (2σ)	37.53349°S, 71.29061°W	2; 3
	CMS	Tuff	Ar/Ar	19.25±1.0 (2σ)	37.53381°S, 71.29076°W	2; 3
	CMS	Tuff	Ar/Ar	19.5±0.6 (2σ)	37.53463°S, 71.29155°W	2; 3
	CMS	Tuff	Ar/Ar	19.80±0.40 (2σ)	37.58177°S, 71.23523°W	2; 3
	CMS	----	Ostracodes	Late Jurassic-Early Cretaceous	~37.71240°S, ~71.35150°W	4
	CMS	----	Freshwater bivalves	Early Eocene	37.70590°S, ~71.3071°W	4
	CMS	----	Freshwater bivalves and gasteropods	Eocene	37.70510°S, 71.28294°W	5
	CMS	----	Ostracodes	Miocene	37.65623°S, 71.23333°W	5
	CMS	----	Mammals	Early-middle Miocene	37.60250°S, 71.23311°W; 37.56776°S, 71.25936°W	3; 6; 7
Río Lileo						
	TT	Tuff	Ar/Ar	10.8±1.6 (2σ)	36.99700°S, 70.96100°W	8
	TT	Tuff	Ar/Ar	11.7±0.3 (2σ)	36.99700°S, 70.96100°W	8
	TT	Tuff	Ar/Ar	16.2±0.2 (2σ)	36.93700°S, 70.71500°W	9; 8
	CMS	Tuff	Ar/Ar	22.8±0.7 (2σ)	37.37100°S, 70.71500°W	9; 8
	CMV	Basalt	Ar/Ar	24.6±1.8 (2σ)	36.88000°S, 71.07900°W	9; 8
Lonquimay						
	MT	Andesite	K/Ar	8.0 ±0.3	38.44034°S, 71.09397°W	10; 12
	MT	Tuff	K/Ar	8.0 ± 0.5	38.63865°S,	10; 12

LOCALITY	UNIT	LITHOLOGY	METHOD	AGE (Ma)	LOCATION	REFERENCE
					71.04166°W	
	MT	Andesite	K/Ar	8.1 ± 0.6	38.60831°S, 71.02162°W	10; 12
	MT	Tuff	K/Ar	8.3 ±0.9	38.44370°S, 71.15709°W	10; 12
	MT	Tuff	K/Ar	8.3 ±0.9	38.60193°S, 71.02575°W	10; 12
	MT	Tuff	K/Ar	9.5 ±2.8	38.61957°S, 71.02165°W	11; 12
	CMS	Andesite	K/Ar	13.0± 1.6	38.45844°S, 71.21196°W	11; 12
	CMS	Tuff	K/Ar	17.5 ± 0.6	38.50686°S, 71.21258°W	11; 12
	CMS	Sandstone	U-Pb	11.6 +0.13-0.08 (m.d.a.) (2σ)	38.63670°S, 71.13180°W	13
	CMS	Sandstone	U-Pb	12.6+0.10-0.17 (m.d.a.) (2σ)	38.58240°S, 71.13860°W	13
	CMS	Sandstone	U-Pb	12.7+0.10-0.08 (m.d.a.) (2σ)	38.62670°S, 71.15890°W	13
	CMS	Sandstone	U-Pb	16.4+0.22-0.15 (m.d.a.) (2σ)	38.57690°S, 71.27940°W	13
	CMS	----	Mammals	Early-late middle Miocene	37.98844°S, 71.44509°W; 38.46128°S, 71.22343°W; 38.50435°S, 71.22154°W; 38.58397°S, 71.13844°W; 38.64017°S, 71°.14581°W	14
	CMV	Tuff	K/Ar	7.8 ± 0.8	38.23645°S, 71.36715°W	11; 12
	CMV	Andesite	K/Ar	10.7± 1.1	38.73557°S, 71.33639°W	11; 12
	CMV	Andesite	K/Ar	11.0 ± 1.6	38.24187°S, 71.34420°W	11; 12

LOCALITY	UNIT	LITHOLOGY	METHOD	AGE (Ma)	LOCATION	REFERENCE
	CMV	Andesite	K/Ar	11.6 ±0.8	38.25077°S, 71.23422°W	11; 12
	CMV	Andesite	K/Ar	11.9±0.8	38.37334°S, 71.35988°W	11; 12
	CMV	Tuff	K/Ar	12.0 ± 1.6	38.18934°S, 71.37962°W	11; 12
	CMV	Intrusive	K/Ar	12.6 ± 0.7	38.30996°S, 71.42987°W	11; 12
	CMV	Monzonite	K/Ar	12.6 ± 0.7	38.32031°S, 71.43022°W	11; 12
	CMV	Andesite	K/Ar	12.8 ± 0.7	38.36284°S, 71.37785°W	11; 12
	CMV	Tuff	K/Ar	12.8 ± 1.6	38.18713°S, 71.37773°W	11; 12
	CMV	Andesite	K/Ar	12.9± 1.5	38.73576°S, 71.32719°W	11; 12
	CMV	Tuff	K/Ar	13.0± 1.7	38.22586°S, 71.35625°W	11; 12
	CMV	Tuff	K/Ar	13.1 ±0.7	38.21560°S, 71.37362°W	11; 12
	CMV	Tuff	K/Ar	13.1 ± 1.7	38.22542°S, 71.35566°W	11; 12
	CMV	Diorite	K/Ar	13.4 ± 1.4	38.24352°S, 71.37396°W	11; 12
	CMV	Breccia	K/Ar	14.1 ± 1.6	38.20577°S, 71.34704°W	11; 12
	CMV	Tuff	K/Ar	14.6 ± 0.5	38.23656°S, 71.38401°W	11; 12
	CMV	Dacite	K/Ar	14.6 ± 1.6	38.20511°S, 71.34616°W	11; 12
	CMV	Monzonite	K/Ar	15.5 ± 0.7	38.22513°S, 71.36983°W	11; 12
	CMV	Andesite	K/Ar	15.5 ± 2.3	38.74351°S, 71.32255°W	11; 12
	CMV	Andesite	K/Ar	16.3±2.1	38.32287°S, 71.33766°W	11; 12

LOCALITY	UNIT	LITHOLOGY	METHOD	AGE (Ma)	LOCATION	REFERENCE
	CMV	Tuff	K/Ar	16.4 ± 2.5	38.21071°S, 71.37004°W	11; 12
	CMV	Andesite	K/Ar	17.2 ± 2.4	38.30490°S, 71.33508°W	11; 12
	CMV	Andesite	K/Ar	18.7±2.1	38.33409°S, 71.35117°W	11; 12
	CMV	Andesite	K/Ar	19.1 ± 2.8	38.12501°S, 71.37525°W	11; 12
	CMV	Andesite	K/Ar	19.9± 1.4	38.42184°S, 71.46569°W	11; 12
	CMV	Andesite	K/Ar	22.0 ± 0.9	38.39189°S, 71.27576°W	11; 12
Agrio and Chos Malal FTBs						
Cerro Naunauco						
	Tralalhue Fm	----	Mammals	Middle Miocene	Not indicated	15
Chos Malal						
	Rincón Bayo Fm.	----	Correlation	Middle-late Miocene(?)	37.41889°S, 70.26583°W	16
	Chos Malal Fm	----	Correlation	Middle Miocene(?)	37.41889°S, 70.26583°W	16
Pampa de Agua Amarga						
	Rincón Bayo Fm.	----	Stratigraphy and	Middle-late Miocene(?)	~37.00294°S, ~69.84064°W	17
	Puesto Burgos Fm.	----	Mammals	Early Miocene	~38.39006°S, ~69.72428°W	18
Sierra de Huantraico						
	La Tiza Fm.	----	Stratigraphy	Late Miocene(?)	37.32369°S, 69.65983°W; 37.56264°S, 69°.93334W	19
	Sierra Negra Fm.	Basalt	Ar/Ar	19.1±0.8	37.41600°S, 69.53283°W	20
	Sierra Negra Fm.	Andesite	Ar/Ar	19.8±0.7	37.59667°S, 69.83333°W	20

LOCALITY	UNIT	LITHOLOGY	METHOD	AGE (Ma)	LOCATION	REFERENCE
	Sierra Negra Fm.	Basalt	K/Ar	22±2	37.68590°S, 70.35080°W	21
	Sierra Negra Fm.	Basalt	K/Ar	21±2	37.58820°S, 70.80790°W	21
	Sierra Negra Fm.	Basalt	Ar/Ar	22.1±0.5	~37.36240°S, ~69.61830°W	22
	Sierra Negra Fm.	Basalt	Ar/Ar	22.2±0.2	~37.22980°S, ~69.85160°W	22
	Sierra Negra Fm.	Basalt	Ar/Ar	23.4±0.4	37.26267°S, 69.65217°W	20
	Sierra Negra Fm.	----	Mammals	Early Miocene	37.41433°S, 69.48225°W; 37.51289°S, 69°54033°W	19
	Rincón Escondido Fm.	----	Mammals	Oligocene	37°.56264°S, 69°.93456°W	19
	Rodados Lustrosos Fm.	----	Correlation	Late Eocene-early Oligocene (?)	37.32369°S, 69.65983°W; 37.56264°S, 69°.93334W	19
Pampa de Carrizalito						
	Tristeza Fm.	----	Stratigraphy	Late(?) Miocene	36.62439°S, 69.91550°W	23; 24; 25
	Palauco Fm.	Andesite	Ar/Ar	18.1±0.24	36.17280°S, 69.57650°W	23; 24; 25
Foreland						
	El Palo Fm.	----	Mammals	Late Miocene-early Pliocene	~38.03768°S, ~69.09157°W	26; 27
	Barranca de los Loros Fm.	----	Mammals	Middle Miocene	~37.16325°S, ~69.79253°W	26; 27
	Chichinales Fm.	----	Mammals	Early Miocene	39.12678°S, 67.76484°W	28
	Vaca Mahuida Fm.	----	Correlation	Late Oligocene-early Miocene	~37.43381°S, ~69.02155°W	27

M.d.a.: maximum depositional age. The localities referenced in the table are illustrated in figures 2 and 3. Figure 3 also indicates the locations of radiometric ages for the CMV, CMS, and Trapa Trapa formations at the Laguna del Laja-Río Lileo area. The references for the compiled ages are as follows: 1) Drake (1976). 2) Herriott (2006). 3) Flynn et al. (2008). 4) O. González and Vergara (1962). 5) Niemeyer and Muñoz (1983). 6) Solórzano et al. (2020). 7) Solórzano et al. (2021). 8) Burns et al. (2006). 9) Jordan et al. (2001). 10) Muñoz (1988). 11) Suárez and Emparán (1995). 12) Suárez and Emparán (1997). 13) Pedroza et al. (2017). 14) Solórzano et al. (2019). 15) Repol et al. (2002). 16) Cervera and Leanza (2009). 17) Leanza et al. (2001). 18) Zamora Valcarce (2007). 19) Garrido et al. (2012). 20) Kay and Copeland (2006). 21) V. A. Ramos and Barbieri (1989). 22) Cobbold and Rossello (2003). 23) Sagripanti et al. (2011). 24) Sagripanti et al. (2012). 25) Silvestro and Atencio (2009). 26) Pascual et al. (1984). 27) Rodríguez et al. (2007). 29) Barrio et al. (1986).

200 meters. This area is predominantly characterized by Plio-Pleistocene fluvial deposits, often with variable thicknesses of up to approximately 2000 meters, which unconformably overlie Paleozoic-Triassic basement rocks as well as Oligocene-Miocene volcanic, nonmarine, and marine rocks (Encinas et al., 2021).

The Principal Cordillera (figs. 2, and 3) reaches maximum elevations of approximately 3000 meters and is home to active volcanoes. The boundary between the Central Depression and the Principal Cordillera is defined by a significant west-vergent reverse fault defined as the West Andean Thrust (WAT) by Armijo et al. (2010). Another noteworthy tectonic feature within the Principal Cordillera is the N–S-oriented dextral strike-slip Liquiñe-Ofqui fault zone (LOFZ), which extends between ~46°–38°S (Hervé, 1994). In south-central Chile, the Principal Cordillera can be further subdivided into a western and an eastern domain based on predominant stratigraphic units. The western domain is characterized by extensive Oligo-Miocene nonmarine volcanic rocks, along with rarer occurrences of Upper Cretaceous and Miocene plutonic rocks, and Plio-Quaternary volcanic rocks (Contreras et al., 2022; Niemeyer & Muñoz, 1983; Spikings et al., 2008; Suárez & Emparán, 1997). The eastern part of the Principal Cordillera is primarily composed of upper Oligocene to upper Miocene nonmarine sedimentary and volcanic rocks, as well as Plio-Pleistocene nonmarine volcanic rocks (Flynn et al., 2008; Folguera et al., 2007; Niemeyer & Muñoz, 1983; Rojas Vera et al., 2016; Suárez & Emparán, 1997). Locally, Upper Cretaceous-Paleocene volcanic rocks and Lower-Middle Jurassic marine sedimentary and volcanic rocks are also exposed (Suárez & Emparán, 1997).

The Agrio and Chos Malal Fold and Thrust Belts (FTBs) are situated to the east of the Principal Cordillera (figs. 2, and 3). The boundary between these two domains is delineated by the Andacollo and Loncopué Fault System (ALFS; Cobbold & Rossello, 2003). This west-vergent thrust system is a prominent geological and topographic feature that separates the Principal Cordillera from the FTBs. To the west of this fault system, Cenozoic sedimentary and volcanic rocks of the Principal Cordillera prevail (Rojas Vera et al., 2016). To the east of the ALFS, the Agrio and Chos Malal FTBs, which typically exhibit higher maximum elevations than the Principal Cordillera, predominantly consist of Jurassic and Cretaceous sedimentary rocks deposited in marine and nonmarine settings within the backarc Neuquén basin. Older Paleozoic, Permian, and Triassic sedimentary and volcanic rocks are exposed on the western flank of the FTBs, particularly in the Cordillera del Viento anticline (Cobbold & Rossello, 2003; Rojas Vera et al., 2016; Sánchez et al., 2018), in addition to Upper Cretaceous to Eocene volcanic and sub-volcanic rocks (Rojas Vera et al., 2016). Small outcrops of upper Oligocene to Miocene volcanic and sedimentary rocks can be found in various areas of the FTBs (Cervera & Leanza, 2009; Garrido et al., 2012; Zamora Valcarce et al., 2006).

The foreland (fig. 2) is a region of low relief, with maximum elevations reaching approximately 1000 meters, gradually diminishing toward the east. The older rocks exposed in this area consist of Upper Cretaceous to lower Paleocene nonmarine and marine rocks (Rodríguez et al., 2007). These are overlain by upper Oligocene to lower Miocene marine strata, which, in turn, are covered by lower Miocene to Pleistocene nonmarine deposits (Rodríguez et al., 2007).

Paleozoic, Mesozoic, Paleogene, and Miocene rocks in the Principal Cordillera and the Agrio and Chos Malal FTBs typically display significant deformation, characterized by tight folding and reverse faulting (Flynn et al., 2008; Niemeyer & Muñoz, 1983; Rojas Vera et al., 2016). These formations are locally covered by subhorizontal Plio-Pleistocene volcanic rocks of the Cola de Zorro Formation and equivalent units (Jordan et al., 2001; Muñoz & Niemeyer, 1984; Niemeyer & Muñoz, 1983; Rojas Vera et al., 2016; Suárez & Emparán, 1995, 1997). In contrast, Upper Cretaceous and Cenozoic rocks in the foreland region generally remain undeformed.

2.2. OLIGOCENE-MIOCENE VOLCANIC AND SEDIMENTARY ROCKS

Oligocene-Miocene volcanic and sedimentary formations are exposed across the Principal Cordillera and the Agrio and Chos Malal FTBs (figs. 2, and 3). The absence of complete sections and the disparity in ages have led to the development of various stratigraphic schemes, making correlations difficult. In the following section, we will review the most significant antecedents of these geological units.

The Cura Mallín Formation was initially defined in the Laguna del Laja area (~37°–38°S; figs. 2, and 3) by O. González and Vergara (1962) as a sedimentary unit with some volcanic intercalations. Subsequently, Niemeyer and Muñoz (1983) subdivided this formation into a lower volcanic Member (Río Queuco) and an upper sedimentary Member (Malla Malla). Afterward, Muñoz and Niemeyer (1984), Suárez and Emparán (1995, 1997), and Jordan et al. (2001) modified earlier stratigraphic schemes and incorporated various Oligocene-Miocene volcanic and sedimentary units, which are exposed in the Principal Cordillera of south-central Chile and Argentina between ~36° and 39°S, into the Cura Mallín Formation (fig. 2).

Given their differing lithologies and in line with the criteria established in the international stratigraphic standard (Harland, 1977), we suggest that the volcanic and sedimentary strata attributed to the Cura Mallín Formation should be acknowledged as separate units. To simplify, we will refer to them as the CMV (Cura Mallín Volcanic) and CMS (Cura Mallín Sedimentary) formations, as previously noted.

Volcanic rocks from the CMV are exposed in the Principal Cordillera, primarily in the western region of this mountain range (figs. 2, and 3). This unit is predominantly composed of andesitic lavas and tuffs and has an estimated thickness of up to ~2000 meters (Muñoz & Niemeyer, 1984). The CMV unconformably overlies Jurassic, Upper Cretaceous, and Paleocene rocks (Muñoz & Niemeyer, 1984; Niemeyer & Muñoz, 1983; Suárez & Emparán, 1995, 1997). The contact between the CMV and the CMS is conformable and has only been observed in a few locations in the eastern Principal Cordillera, including the Río Lileo area in Argentina (~37° S; Espinach, 2009; Utgé et al., 2009) and the

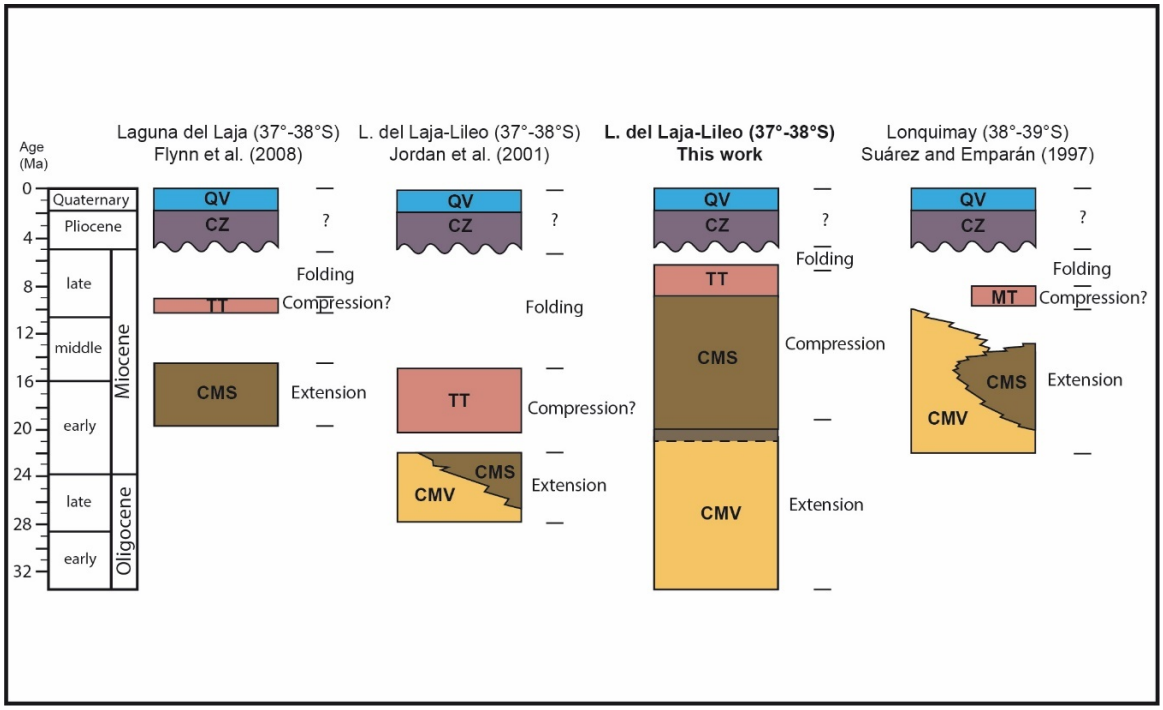

Figure 4. Chronostratigraphic chart illustrating different stratigraphic schemes, age, and tectonic interpretations for the Cura Mallín (CMV and CMS), Trapa Trapa, and Mitrauquén formations in the Laguna del Laja, Río Lileo and Lonquimay areas.

The age ranges are determined based on radiometric ages (K/Ar, Ar/Ar, and U-Pb) sourced from Suárez and Emparán (1997), Jordan et al. (2001), Flynn et al. (2008), and the current study, as depicted in table 1, figure 5, and figure 6. Note the significant differences in the age ranges of the CMS and Trapa Trapa Formation between Jordan et al.'s (2001) scheme and those proposed by other authors. Compare this stratigraphic chart with those published in Flynn et al. (2008, their fig. 6) and Melnick et al. (2006, their fig. 2). CMV: Cura Mallín Formation volcanic rocks. CMS: Cura Mallín Formation sedimentary rocks. TT: Trapa-Trapa Formation sedimentary and volcanic rocks. CZ: Plio-Pleistocene basalts of the Cola de Zorro Formation and equivalent units. QV: Quaternary volcanic rocks.

Lonquimay area in Chile (~39°S; Encinas et al., 2022; Pedroza et al., 2017).

The age of the CMV was originally assigned to the lower-middle Miocene by Drake (1976), who obtained four K/Ar ages for this unit in the Laguna del Laja area (table 1). However, Muñoz and Niemeyer (1984) argued that the three older dates from Drake's work actually corresponded to volcanic rocks of the Trapa Trapa Formation. Since Drake (1976) did not clearly indicate the sample locations, they are not considered in this study. Most K/Ar, Ar/Ar, and U-Pb radiometric ages for volcanic rocks attributed to the CMV and equivalent units in the region fall within the Eocene to lower Miocene range (table 1; Contreras et al., 2022; Encinas et al., 2022; Jordan et al., 2001; Vergara et al., 1999), allowing for correlation with the Abanico Formation located north of 36°S (Charrier et al., 1996, 2002). However, Suárez and Emparán (1997) reported K/Ar ages from the middle to late Miocene for volcanic rocks in the western Principal Cordillera (figs. 4, and 5, and table 1). They tentatively attributed these rocks to the CMV, while acknowledging that part of them likely belong to younger units.

Sedimentary rocks of the Cura Mallín Formation (CMS) are exclusively exposed in the eastern Principal Cordillera in Chile and Argentina. The CMS Formation has an estimated maximum thickness of approximately 1900 meters in Chile (Herriott, 2006) and 2500 meters in Argentina (Gutiérrez & Minniti, 1985). It consists of conglomerate, sandstone, siltstone, and minor limestone and tuff, which were deposited in fluvial, lacustrine, and deltaic environments (Muñoz & Niemeyer, 1984; Niemeyer & Muñoz, 1983; Suárez & Emparán, 1995). The CMS Formation conformably overlies the volcanic rocks of the CMV and exhibits a conformable contact or a disconformity with the overlying Trapa Trapa Formation (Burns et al., 2006; Niemeyer & Muñoz, 1983).

The age of the CMS Formation, originally ascribed to the Jurassic-Cretaceous based on ostracods (O. González & Vergara, 1962), or to the Eocene based on freshwater bivalves (Niemeyer & Muñoz, 1983), has been a subject of debate. Subsequent studies conducted various K/Ar, Ar/Ar, and U-Pb radiometric analyses on volcanic and sedimentary strata within the CMS Formation, resulting in age determinations spanning the early, middle, and late Miocene (figs 4, and 5, and table 1; Encinas et al., 2022; Flynn et al., 2008; Herriott, 2006; Pedroza et al., 2017; Suárez & Emparán, 1995). These ages are supported by distinct mammalian assemblages, ranging from the Colhuehuapian (early Miocene) to potentially the Mayoan (late middle Miocene) SALMAs (Flynn et al., 2008; Solórzano et al., 2019, 2020, 2021, 2023).

In contrast, Jordan et al. (2001) proposed a late Oligocene–early Miocene age for the CMS Formation, based on an Ar/Ar age of 22.8 Ma from the upper part of this unit in the Río Lileo area (Argentina). Using this age and another Ar/Ar age of 24.6 Ma for the basal part of the CMV in the same area, they suggested that both units are con-

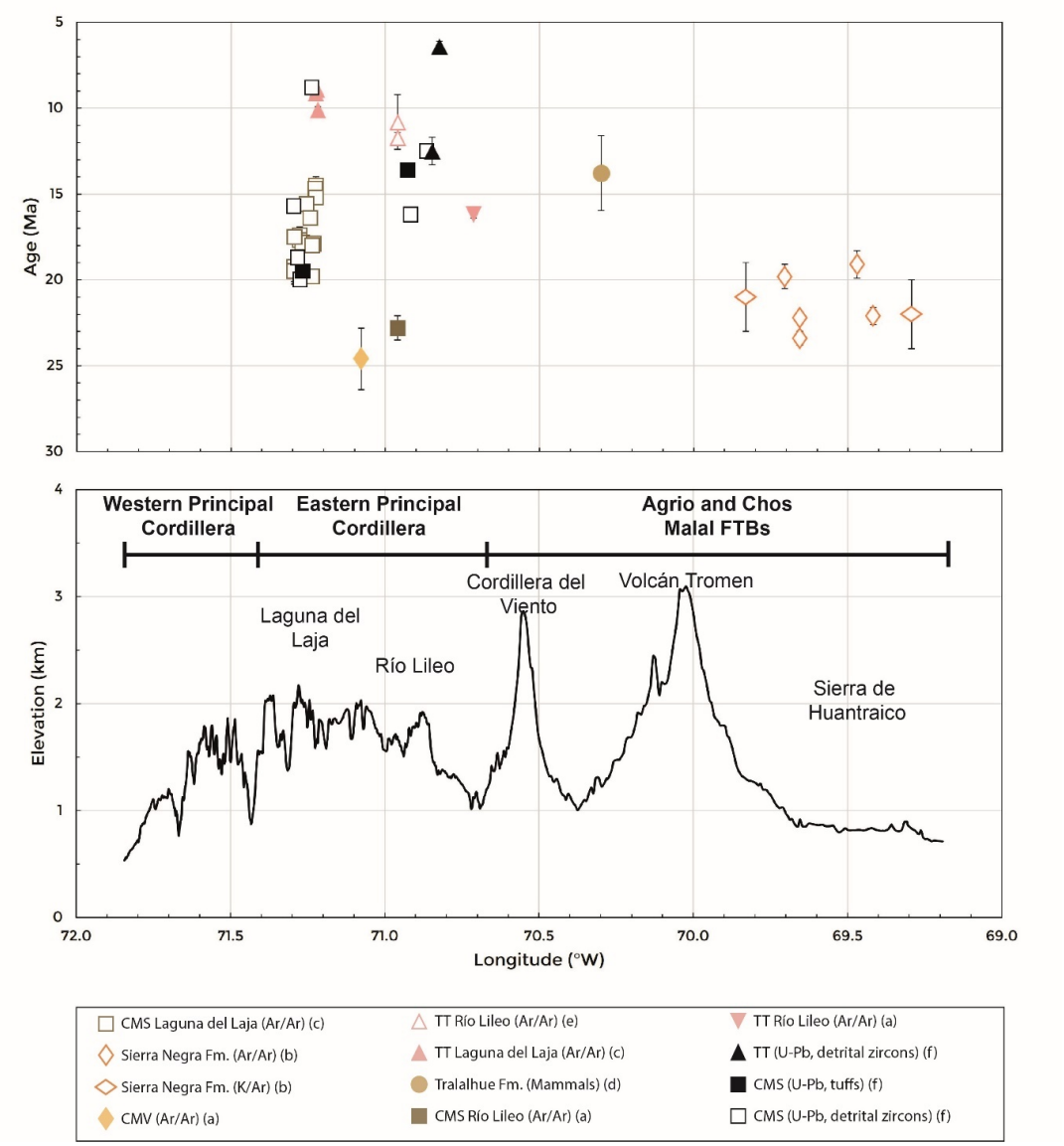

Figure 5. East-west transect across the Principal Cordillera and the Agrio-Chos Malal FTBs at the latitudes of the study area (see location of profile A–A' in figure 2).

The transect showcases radiometric (Ar/Ar and U-Pb) and mammal ages from various sources: a) Jordan et al. (2001), b) Garrido et al. (2012) and references therein, c) Herriott (2006) and Flynn et al. (2008), d) Repol et al. (2002), e) Burns et al. (2006), and f) this study. For more detailed information about the ages and localities, see table 1 and figures 3 and 7. Note the discordance between the 22.8 Ma Ar/Ar age reported by Jordan et al. (2001) for the CMS and those from Herriott (2006), Flynn et al. (2008), and the present study for the same unit. Also discordant is the Ar/Ar age of 16.2 Ma from Jordan et al. (2001) for the Trapa Trapa Formation with those from Herriott (2006), Flynn et al. (2008), Burns et al. (2006), and this study for the same unit. TT: Trapa Trapa Formation.

temporaneous and laterally equivalent (figs. 4, and 5, and table 1). A similar interpretation was presented by Suárez and Emparán (1995, 1997) for the Lonquimay area. They argued that the CMV (their Guapitrío Member) and CMS (their Río Pedregoso Member) formations are also contemporaneous and laterally equivalent, based on early to middle-late Miocene K/Ar ages for both units (figs. 4, and 5, and table 1). However, the oldest age reported for the Guapitrío Member (22.0 Ma) by these authors was obtained from a location where Pedroza et al. (2017) and Encinas et al. (2022) observed a contact between this unit and the overlying Río Pedregoso Member (CMS). It is likely that the younger ages obtained from volcanic rocks in the western Principal Cordillera correspond to younger units (Suárez & Emparán, 1997), as indicated before.

To the east of the Principal Cordillera, the Agrio and Chos Malal FTBs are primarily composed of Jurassic and Cretaceous rocks (figs. 2 and 3). Cenozoic strata are relatively rare, but Oligocene-Miocene volcanic and nonmarine sedimentary rocks are found in limited outcrops, typically corresponding to elevated synclines (figs. 2 and 3). The volcanic rocks of the Palaoco and Sierra Negra formations, reaching thicknesses of up to 850 meters, are characterized by andesite, basalt, breccia, and tuff. Various K/Ar and Ar/Ar dating methods have provided late Oligocene to early Miocene ages for these rocks (fig. 5, and table 1; Cobbold & Rossello, 2003; Kay & Copeland, 2006; V. A. Ramos & Barbieri, 1989; Sagripanti et al., 2011; Silvestro & Atencio, 2009), suggesting a probable correlation with the CMV.

Nonmarine conglomerate, sandstone, siltstone, and minor tuff, with a thickness of approximately 400 m, are found in the Tralalhue Formation and equivalent units. These rocks unconformably overlie Cretaceous, Paleocene strata, or upper Oligocene-lower Miocene volcanic rocks of the CMV (Cervera & Leanza, 2009; Leanza et al., 2001; V. A. Ramos, 1998; Zamora Valcarce et al., 2006). Mammal fossils indicate early to middle Miocene ages for these units (fig. 5, and table 1; Repol et al., 2002; Zamora Valcarce, 2007).

The Trapa-Trapa Formation was defined by Niemeyer and Muñoz (1983) in the Laguna del Laja area (fig. 3). This unit can reach thicknesses of up to 1500 meters and consists of cobble to boulder conglomerates interbedded with andesitic to basaltic lavas and volcanic breccia. Equivalent units in the Río Lileo area in Argentina were assigned to this formation by Jordan et al. (2001). The Trapa Trapa Formation exhibits a concordant contact with the CMS and an angular unconformity with the Pliocene-Pleistocene volcanic rocks of the Cola de Zorro Formation and equivalent units (Jordan et al., 2001; Muñoz & Niemeyer, 1984; Niemeyer & Muñoz, 1983; Suárez & Emparán, 1995, 1997). Jordan et al. (2001) initially assigned a late early Miocene age to this unit, based on an Ar/Ar age of 16.2 Ma in the Río Lileo area. However, subsequent studies by Burns et al. (2006) and Flynn et al. (2008) yielded additional Ar/Ar late middle to late Miocene ages for the same unit in the Río Lileo and Laguna del Laja areas respectively (figs. 3, 4, and 5, and table 1).

The Mitrauquén Formation, characterized by a succession of conglomerates, ignimbrites, and minor andesitic lavas with a thickness of up to 300 meters, is exposed in the Lonquimay area (fig. 2; Suárez & Emparán, 1997; Zanettini et al., 2010). Herriott (2006) correlated this formation with the Trapa Trapa Formation. Muñoz (1988) and Suárez and Emparán (1997) dated ignimbrites within this unit and obtained late Miocene K/Ar ages (table 1).

3. U-PB GEOCHRONOLOGY

Jordan et al. (2001) assigned a late Oligocene–early Miocene age for the CMS and a late early Miocene age for the Trapa Trapa Formation in the Río Lileo area. In contrast, Flynn et al. (2008) determined early to middle Miocene ages for the former and late Miocene ages for the latter in the Río Laja area (fig. 3). Therefore, resolving these uncertainties and establishing reliable correlations between these units and other Oligocene-Miocene formations in the Andes of south-central Chile and Argentina is crucial. To address this, we obtained the first U-Pb ages (10 samples) from sedimentary and volcanic rocks of the CMS and Trapa Trapa formations in the Laguna del Laja-Río Lileo areas (figs. 3, 6, and 7, and table S1).

3.1. ANALYTICAL METHOD

We conducted U-Pb geochronology on 10 samples, comprising 8 from the CMS and 2 from the Trapa Trapa Formation. To determine the depositional ages of volcanic rocks and maximum depositional ages, as well as the zircon provenance of sedimentary rocks, we analyzed more than 50 and over 100 zircon crystals per sample, respectively. The calculated $^{206}U/^{238}Pb$ Tuff Zirc ages and other age groups are detailed in table S1 and figures 6 and 7. The geographic sample locations are illustrated in figure 3.

Zircon concentrates from all samples were separated at the Zirchron LLC laboratory in Tucson, Arizona. Each sample was unpacked, and pressure washed with water to remove any debris and/or foreign materials. The sample rock fragments were introduced into the sample chamber of an Electro Pulse Disaggregator (EPD, Marx generator), where electrical pulses were applied at a 1–2 Hz repetition rate and discharges of ~220 kV for 15 minutes. The material, ranging in size from 500 µ to 25 µ, was subsequently processed using traditional techniques involving the Wilfley water table, Frantz paramagnetic separator, and a one-step (3.32 gm/cc) heavy liquid MEI separation. Zircons from the non-magnetic fraction were mounted together with standards in a 1-inch diameter epoxy puck and polished following standard laboratory procedures.

After performing cathodoluminescence imaging, we conducted U-Pb analyses using laser ablation ICP-MS at Washington State University. We utilized an Analyte G2 193nm excimer laser connected to the Element2 high-resolution inductively coupled plasma mass spectrometer. For the U-Pb measurements, our methodology closely followed that of Chang et al. (2006), with the exception of using the 193nm laser instead of the 213nm laser. The laser parameters for the U-Pb analyses included a spot size ranging from 25 to 35 µm, a repetition rate of 10 Hz with a power of approximately 5 J/cm2. He and Ar carrier gases delivered the sample aerosol to the plasma. Each analysis consisted of a short blank analysis followed by 250 sweeps through masses 202, 204, 206, 207, 208, 232, 235, and 238, taking approximately 30 seconds in total. Unknowns were run in sets of 10 analyses bracketed by standards. Data processing was conducted offline using the Iolite software (Paton et al., 2010). U and Th concentrations were monitored by comparison to the zircon standards 91500 Plesovice (Sláma et al., 2008), FC-1 (Paces & Miller, 1993), and Fish Canyon Tuff, with an age of 28.4 Ma (Schmitz & Bowring, 2001). Common Pb correction was applied using the ^{207}Pb method (Williams, 1998). U-Pb diagrams and ages were calculated using Isoplot (Ludwig, 2003).

Interpreted ages are determined based on $^{206}Pb/^{238}U$ for grains younger than 1200 Ma and $^{206}Pb/^{207}Pb$ for grains older than 1200 Ma. Additionally, a soft filter of 30% was applied to rocks older than the Mesozoic. U-Pb zircon maximum deposition age errors are reported by calculating the quadratic sum of the analytical error and the total systematic error for the set of analyses (Valencia et al., 2005). Interpretations for detrital zircons are established using representative groups, which are those with three or more overlapping zircon ages (Gehrels et al., 2006). The maximum depositional age was calculated using the TuffZirc algorithm (Ludwig, 2003) from the youngest cluster ages (>6) that overlap within a 2σ error range. Zircons from the sandstone samples are clear, colorless, and exhibit various morphologies, primarily as long euhedral crystals. Mi-

nor proportions of subhedral to subrounded zircon crystals are also present. Zircons from the tuffs are clear, pink, long euhedral crystals with prominent bi-pyramidal terminations. Cathodoluminescence images reveal a straightforward growth history characterized by oscillatory to sector zoning.

3.2. POTENTIAL SEDIMENT SOURCES

Three potential sediment sources for the CMS and Trapa Trapa formations include the Coastal Cordillera, the western Principal Cordillera, and the Agrio and Chos Malal FTBs (figs. 2 and 3).

The Coastal Cordillera (fig. 2) and the basement of the Central Depression are primarily composed of upper Paleozoic-Triassic metamorphic rocks and Carboniferous-Permian plutonic rocks (Sernageomin, 2003). Some coastal areas feature upper Cretaceous, Paleocene-Eocene, and Neogene marine rocks (García, 1968; Stinnesbeck, 1986). Oligocene-lower Miocene volcanic rocks can be found in certain sections of the Central Depression (Muñoz et al., 2000).

The western Principal Cordillera (figs. 2, and 3) in the study area latitudes comprises extensive Oligo-Miocene volcanic rocks and Miocene plutonic rocks (Niemeyer & Muñoz, 1983; Spikings et al., 2008). Upper Cretaceous plutonic rocks are exclusive to the north (36°S, Spikings et al., 2008) and south (39°S, Suárez & Emparán, 1997) of the study area. However, it is not ruled out that some intrusive rocks at 37°–38°S may have a Late Cretaceous age due to the limited availability of radiometric data.

The Agrio and Chos Malal FTBs (figs. 2, and 3) are characterized by the prevalence of marine and nonmarine sedimentary rocks, as well as rarer volcanic rocks of Jurassic and Cretaceous ages (Rojas Vera et al., 2016). In the Cordillera del Viento, which marks the boundary with the eastern Principal Cordillera, Paleozoic, Permian, and Triassic sedimentary and volcanic rocks crop out (Cobbold & Rossello, 2003; Rojas Vera et al., 2016; Sánchez et al., 2018). Upper Cretaceous to Eocene volcanic and sub-volcanic rocks are exposed principally in the western part of this domain (Rojas Vera et al., 2016). Small outcrops of upper Oligocene to Miocene volcanic and sedimentary rocks can be found scattered throughout the Agrio and Chos Malal FTBs (Cervera & Leanza, 2009; Garrido et al., 2012; Zamora Valcarce et al., 2006).

In summary, the Coastal Cordillera is predominantly composed of upper Paleozoic-Triassic metamorphic and plutonic rocks, the western Principal Cordillera is characterized mainly by Oligo-Miocene igneous rocks, and the Agrio and Chos Malal region is dominated by Paleozoic, Mesozoic, and Paleogene sedimentary and volcanic rocks. Sedimentary and metamorphic rocks in these domains are expected to contain older recycled zircons.

3.3. RESULTS

The analyzed samples comprise sandstone (6 samples), tuff (2 samples), sandy tuff (1 sample), and tuffaceous sandstone (1 sample) (fig. 6, and 7). We obtained three samples from the Cerro Campamento section, located in the Laguna del Laja area (fig. 3, 8, and 9). These samples, from bottom to top, are identified as CAMP-1, CAMP-3, and ECZ-1. CAMP-1 (n=130) is a sandstone representing the basal part of the CMS in the Laguna del Laja area (Flynn et al., 2008). This sample yielded a maximum depositional age of 20.0 ± 0.3 Ma, along with minor age groups ranging from 126 to 175 Ma (n=10) and isolated grains at 42, 86, and 105 Ma. CAMP-3 (n=142) was collected from a 10 m thick ignimbrite, resulting in an age of 19.5 ± 0.3 Ma, and an additional single zircon of 103 Ma. ECZ-1 (n=80) is a sandy tuff obtained from syncontractional growth strata (fig. 9). This sample yielded a maximum depositional age of 18.7 +0.4/−0.5 Ma, along with additional age groups, including 50 Ma (n=1), 87–91 Ma (n=2), 108–122 Ma (n=10), 165–202 Ma (n=12), 245–306 Ma (n=27), and 1059 Ma (n=1).

The sample BNIT-1 (n=92) was collected from folded sandstones underlying an intraformational unconformity at Baños Nitrao (figs. 3, 6, 7, and 10). This sample provided a maximum depositional age of 15.7 +0.2/−0.3 Ma. Zircon grains predominantly exhibited ages from the Miocene to the late Oligocene (14 to 25 Ma), with one isolated grain of 99 Ma.

Sample BULD16-1 is a sandstone from a fluvial succession belonging to the upper CMS in the Río Trapa-Trapa area (fig. 3). These beds display a conformable contact with overlying coarse-grained conglomerates and andesites of the Trapa Trapa Formation (Niemeyer & Muñoz, 1983). This sample yielded a TuffZirc maximum depositional age of 8.8 +0.2/−0.3 Ma, along with additional zircon groups, including 14–20 Ma (n=20), 86 Ma (n=1), 109 Ma (n=2), and 185 Ma (n=1).

We acquired two samples from the upper part of a fluviolacustrine succession of the CMS in the Río Lileo section in Argentina (fig. 3). These sampled beds contain syncontractional growth strata and exhibit a disconformity with upper Miocene volcanic rocks of the Trapa Trapa Formation (fig. 11). The lower sample (RL-1; n=61) corresponds to a tuffaceous sandstone that yielded a TuffZirc maximum depositional age of 16.2 +0.2/−0.4 Ma, with minor age peaks of 82–85 Ma (n=11) and 101–167 Ma (n=8). Sample RL-2 (n=101) is a tuff that provided a TuffZirc age of 13.6 ± 0.2 Ma. All zircon grains in this sample predominantly exhibited ages from the middle Miocene to the late Oligocene (12 to 25 Ma).

We collected a CMS sample from a succession of lacustrine sandstone and siltstone along the Río Reñileuvú in Argentina (fig. 3). In this area, CMS strata exhibit a distinct angular unconformity with younger Plio-Pleistocene basalts (fig. 12c). We sampled a sandstone bed (17CMB-1) that yielded a maximum depositional age of 12.5 +0.3/−0.2 Ma, with minor peaks ranging from 13–23 Ma (n=22), 45 Ma (n=2), 63–69 Ma (n=6), and isolated grains with ages from 109 to 2045 Ma.

In a nearby locality also along the Río Reñileuvú (fig. 3), we obtained two additional samples from a highly deformed succession of fluvial pebble conglomerate and minor sandstone, corresponding to the Trapa Trapa Formation (fig. 12f). The conglomeratic succession displays a tectonic con-

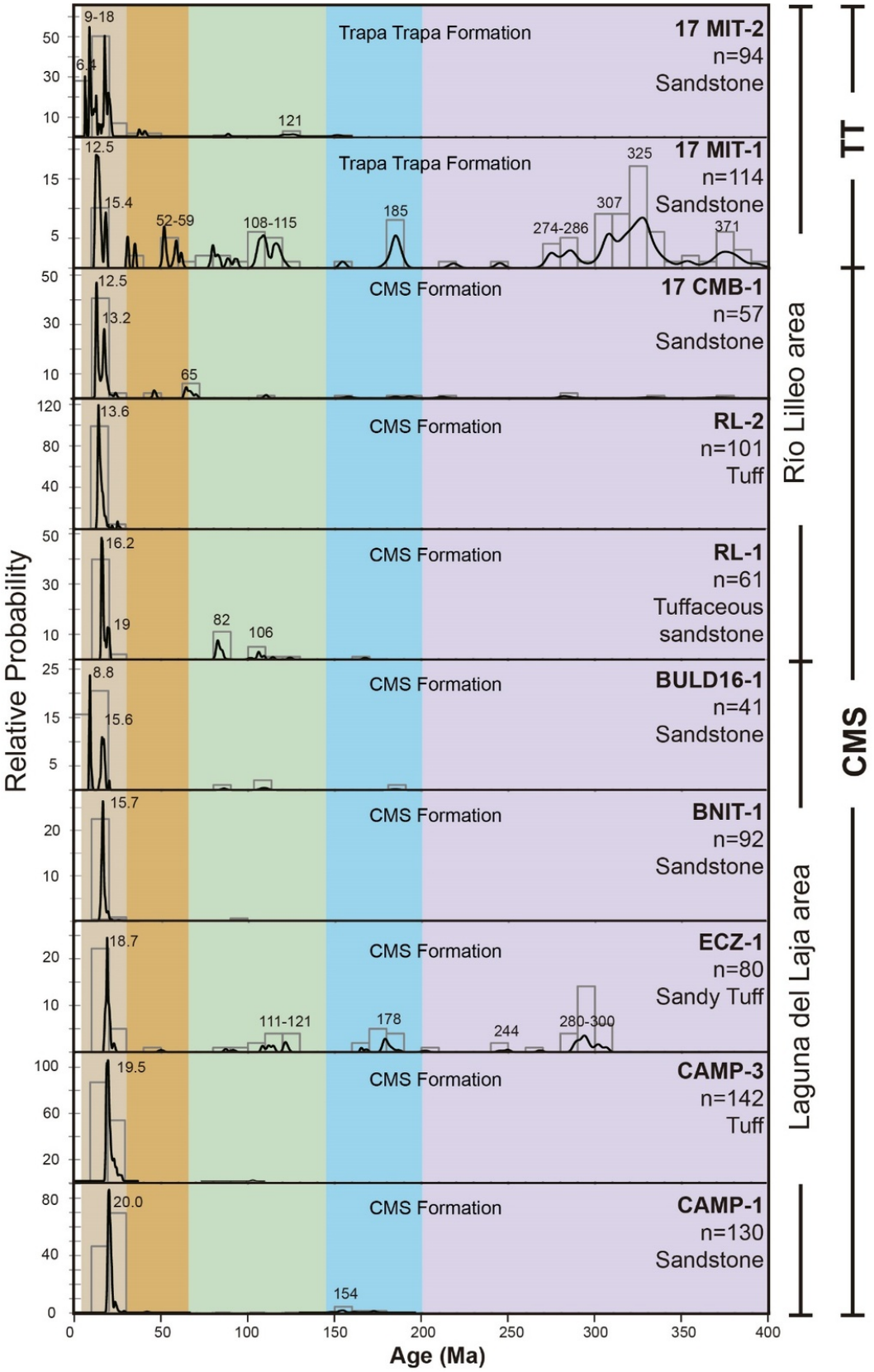

Figure 6. Frequency histograms and relative probability density plots for the U–Pb ages of the CMS and the Trapa Trapa Formation (TT) from the Laguna del Laja and Río Lileo areas.

The sample locations are indicated in figure 3. Colors represent different age ranges: Oligocene-Miocene (brown), Paleocene-Eocene (orange), Cretaceous (green), Jurassic (blue), and Triassic-Paleozoic ages.

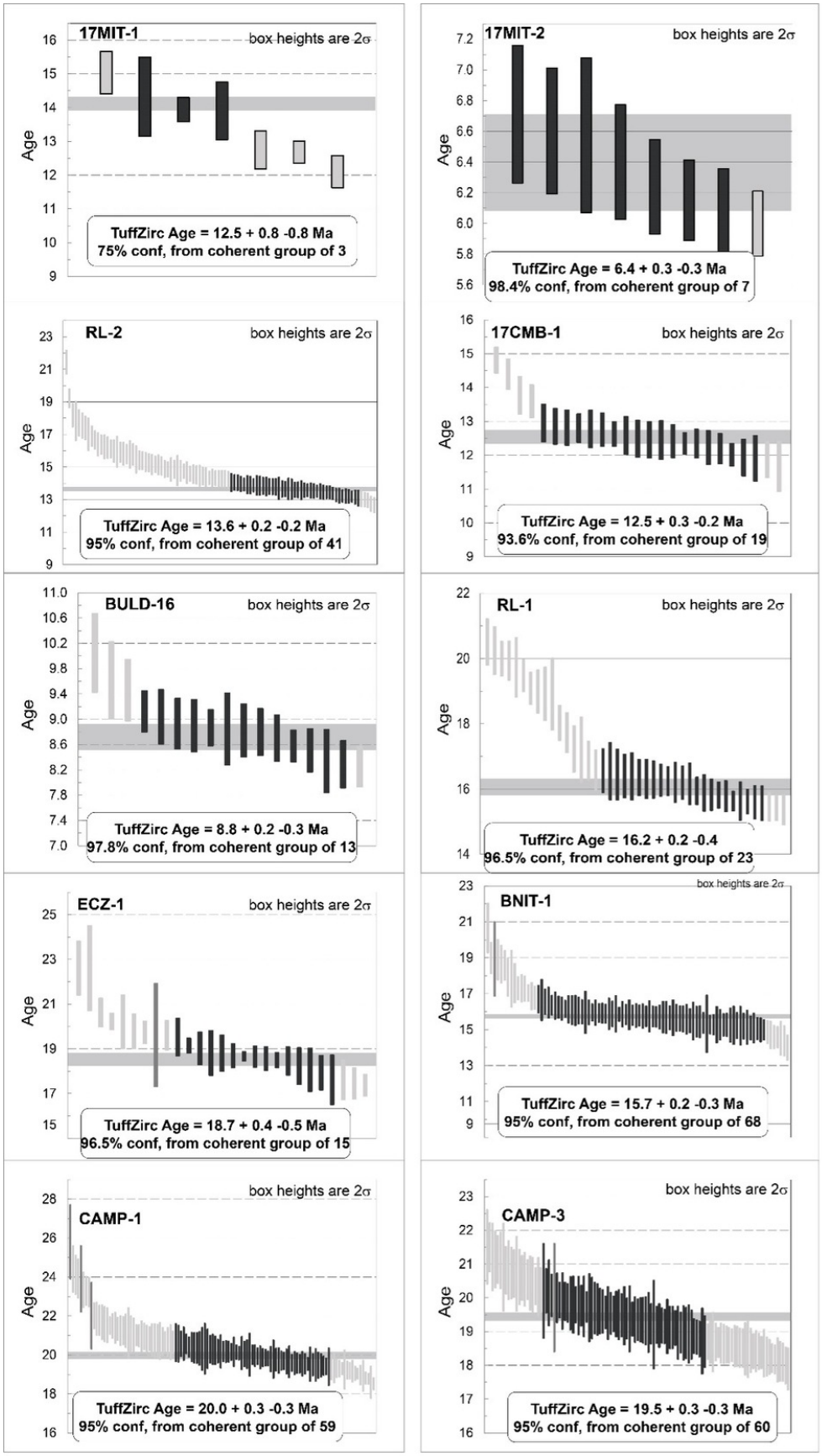

Figure 7. U-Pb ages calculated using the TuffZirc method (Ludwig & Mundil, 2002) for the samples presented in figure 6 and table S1.

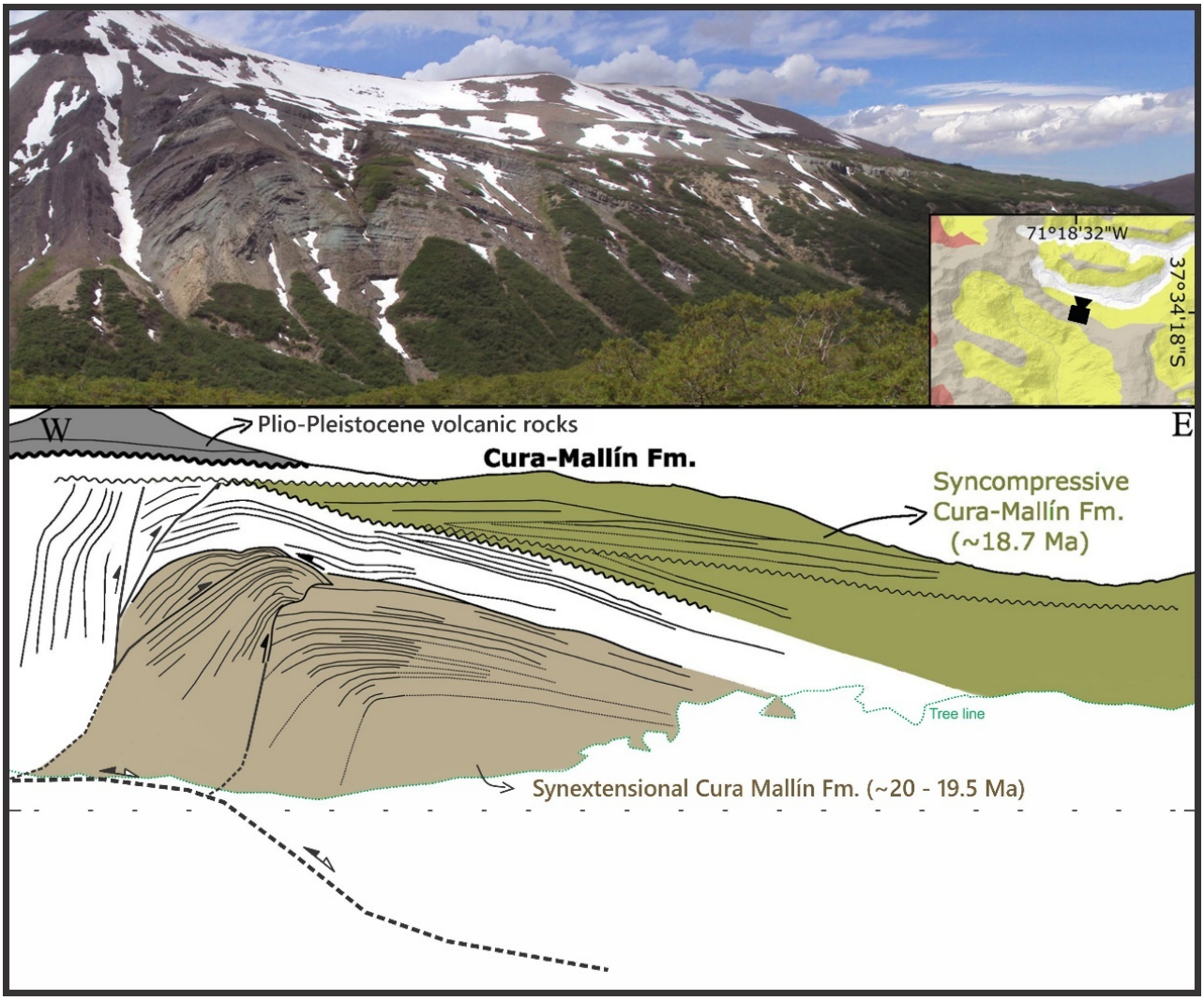

Figure 8. CMS outcrop displaying fan-shaped strata geometry interpreted as an inverted half-graben near Cerro Campamento (Laguna del Laja area, figure 3).

The structure corresponds to a wedge that inserts and propagates within the overlying strata, generating an asymmetric anticline and a series of passive roof faults on the western side, accommodating the deformation of the western frontal flank with steeply inclined layers. Note the onlap relationship between the inverted half-graben and the top of the CMS syn-contractional section.

tact with the CMS, and both units are overlain with angular unconformity by Plio-Pleistocene basalts. Sample 17MIT-1, a sandstone from the basal part of the succession, exhibits highly heterogeneous ages. Three zircon grains provided a maximum depositional age of 12.5 ± 0.8 Ma, with different peaks at 13–18 Ma (n=7), 31–35 Ma (n=2), 52–59 Ma (n=6), 80–93 Ma (n=5), 108–115 Ma (n=11), 185 Ma (n=7), 274–285 Ma (n=11), 304–330 Ma (n=32), and 370 Ma (n=8). Sample 17MIT-2, a sandstone from the upper part of the same succession, yielded a maximum depositional age of 6.4 ± 0.3 Ma, with a significant peak ranging from 8 to 20 Ma (n=71) and minor peaks at 40 Ma (n=4), 120 Ma (n=4), and 151 Ma (n=1).

4. STRUCTURAL DATA

4.1. EVIDENCE OF SYNDEPOSITIONAL DEFORMATION IN THE CMS

To determine the tectonic setting of the CMS, we provide evidence of syndepositional deformation, encompassing both synextensional and syncontractional features that developed during the deposition of this unit.

4.1.1. LAGUNA DEL LAJA

We identified a ~300 m thick inverted extensional wedge in the basal CMS at Cerro Campamento, in the Laguna del Laja area (fig. 3). The wedge-like strata are in close proximity to and are laterally correlative with those beds where we obtained U-Pb samples CAMP-1 (<20.0 Ma) and CAMP-3 (19.5 Ma) (figs. 3 and 8). We interpret this wedge as having formed due to extensional tectonics and subsequently inverted. Younger strata exhibiting internal discordances

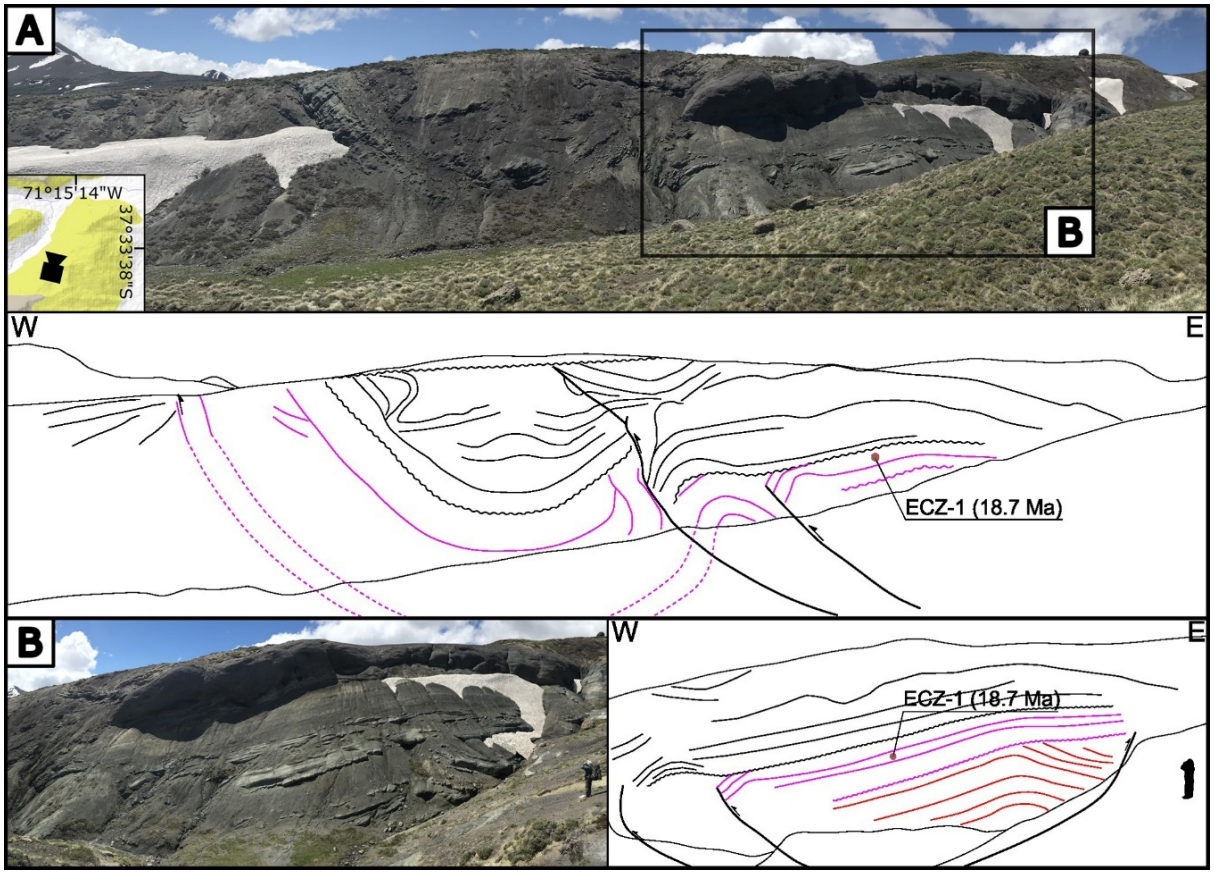

Figure 9. CMS outcrop in Cerro Campamento, Laguna del Laja area (fig. 3).

A) Field photograph and interpretation of CMS syn-contractional strata dated by U-Pb to <18.7 Ma (sample ECZ-1). B) The zoomed-in view highlights three sets of concordant folded strata, separated by intraformational post-deformation erosional unconformities. The lower set forms part of an east-vergent structure (red), which is erosionally truncated by overlying strata (pink). The uppermost set of strata, sitting in erosional and angular unconformity, is also folded (black).

constitute an intraformational angular unconformity that onlaps the top of the inverted synextensional wedge (fig. 8). In a nearby outcrop to the east (fig. 3), equivalent rocks exhibit successive internal folding and internal erosional unconformities (fig. 9). These mesoscale fault-bounded folds were generated by contractional deformation and eroded shortly after their formation. The ECZ-1 sample (<18.7 Ma; fig. 6, 7) was collected from a bed located between the aforementioned unconformities (fig. 9). These strata were deposited at the onset of the contractional tectonic regime that affected the inner Andean sector, which, based on the age of the ECZ-1 sample, commenced in this region around 19 Ma.

At Baños Nitrao, near the Río Trapa-Trapa (fig. 3), we encountered folded strata beneath an angular and erosional intraformational unconformity (fig. 10). We observed eroded hinges in several of these folds, which are indicative of contractional features. Furthermore, we have identified wedge-like growth strata along the fold limbs (as depicted in gray in fig. 10). A detrital zircon sample (BNIT-1) extracted from a sandstone layer within the folded strata provides a maximum depositional age of 15.7 Ma for the folding and associated contractional deformation in this region (figs. 6 and 7).

4.1.2. RÍO LILEO

In the uppermost levels of a ~2,500 m lacustrine and fluvial succession within the CMS at Río Lileo (fig. 3), we observed a progressive decrease in bedding dip toward the top of the succession. The strata exhibit a fan geometry, with dip values decreasing from 60°W to 15°W (fig. 11). These variations in stratal dip are coincident with facies change from sandstone to conglomerate. The Trapa Trapa volcanic rocks exhibit a disconformity overlying the sedimentary rocks of the CMS. In this section, we obtained two U-Pb samples (fig. 11): the lower sample (RL-1) with an age of <16.2 Ma and the upper sample (RL-2) with an age of 13.6 Ma (figs. 6 and 7).

4.2. POST-DEPOSITIONAL DEFORMATION IN THE CMS AND TRAPA TRAPA FORMATIONS

Although we did not conduct a detailed structural analysis of the CMS and Trapa Trapa formations, we observed that these units exhibit intense folding and local faulting in the Laguna del Laja and Río Lileo areas (fig. 12 A–F). Some of the folds are west-vergent, such as the spectacular Cerro Los Pinos anticline-syncline fold pair in the Laguna del Laja area (fig. 12A; see also Carpinelli, 2000; Flynn et al., 2008; O. González & Vergara, 1962). Likely associated with this

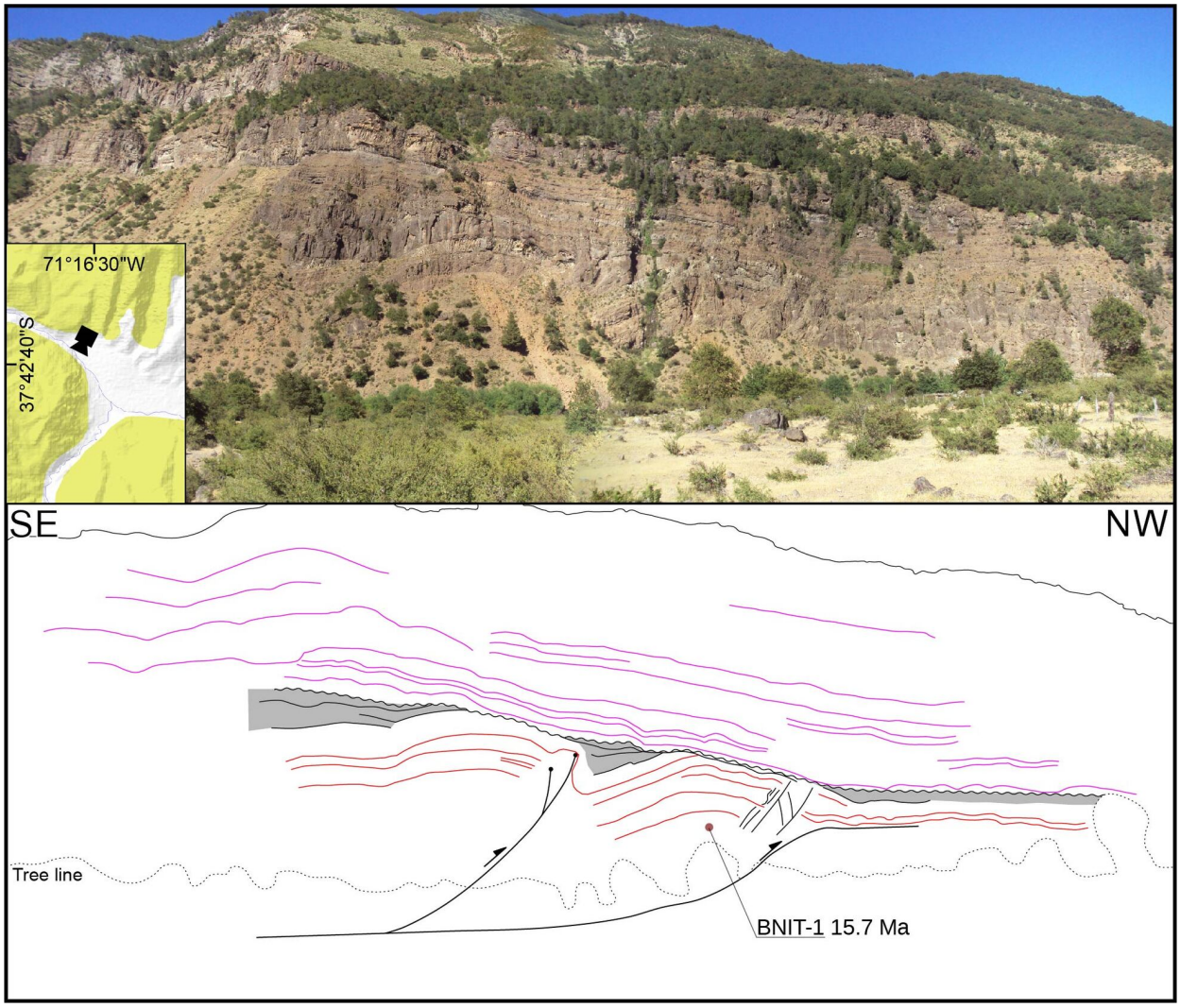

Figure 10. Field photograph and interpretation of CMS strata at the Baños Nitrao locality in the Trapa-Trapa river valley, Laguna del Laja area (fig. 3).

Note the three strata groups corresponding to pre-, syn-, and post-growth successions. In the lower part, strata are affected by two NW-vergent fold-bend-fault anticlines (red lines), with a U-Pb maximum depositional age of <15.7 Ma (sample BNIT-1). Overlying this part, a set of syn-growth strata (gray color) shows lateral thickness variations above the pre-growth strata (red color). Finally, the upper strata lie on top of an erosional intraformational discontinuity, conforming to a monocline (pink color).

fold pair is a tight chevron anticline developed in the CMS west of the Río Trapa-Trapa (fig. 12B) and a west-vergent asymmetric fold within conglomeratic strata of the Trapa Trapa Formation (fig. 12D). An angular unconformity between the CMS and Trapa Trapa formations with the Plio-Pleistocene basalts of the Cola de Zorro Formation, and its equivalent units, marks the conclusion of major deformation in the area (fig. 12C).

5. PALEOCURRENT ANALYSIS OF THE TRAPA TRAPA FORMATION

Encinas et al. (2022) conducted a paleocurrent analysis on imbricated clasts from the Mitrauquén Formation in the Lonquimay area. Their findings revealed unexpected westward transport directions, contradicting the previously proposed western source area by Suárez and Emparán (1997) based on clast composition analysis of this unit. To investigate further, we conducted a similar analysis on the equivalent Trapa Trapa Formation at Laguna del Laja. In the vicinity of the ski resort (fig. 3), we encountered a ~80 m thick succession comprising andesites (10 m), cobble to boulder fluvial conglomerates (30 m), and volcanic breccias (40 m), from the base to the top. The conglomerates are clast-supported, with moderately to well-rounded clasts ranging from decimeters to occasionally exceeding 1 meter in diameter (fig. 13A, B). We performed paleocurrent measurements on imbricated clasts from these beds for two primary reasons. First, the transportation of such large clasts necessitates high energy and is unlikely to be the result of secondary divergent flow. Second, the strata exhibit significant dip values (50°) and are well-lithified, which enhances differential erosion and provides a robust 3D perspective for paleocurrent measurements.

We conducted clast orientation measurements in the field using FieldMove software (Petroleum Experts Ltd.) on an iPad device. Imbricated clasts from three different beds were included in our measurements. Additionally, we

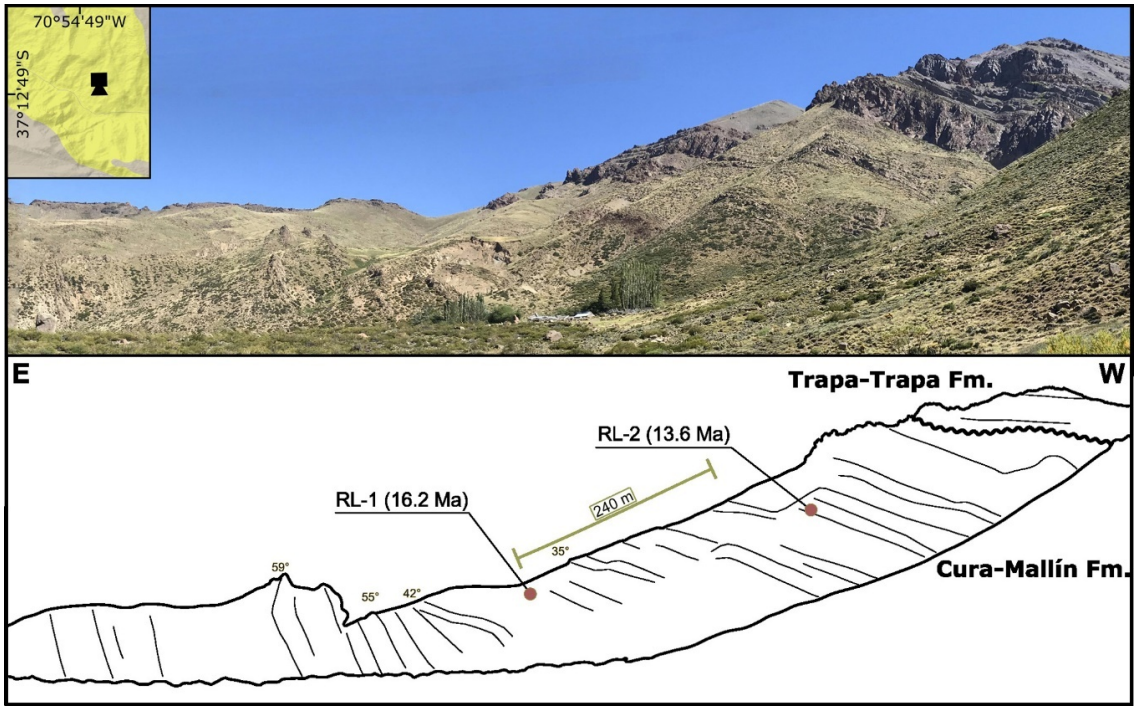

Figure 11. Field photograph illustrating fan geometry in strata of the CMS at Río Lileo (fig. 3).

Two U-Pb samples were collected in this section: the lower one (RL-1) is a tuffaceous sandstone with an age of <16.2 Ma, and the upper one (RL-2) is a tuff with an age of 13.6 Ma. Volcanic rocks of the Trapa Trapa Formation display a disconformity with the CMS.

recorded bedding attitudes to restore paleocurrent data using Stereonet software (Allmendinger et al., 2011; Cardozo & Allmendinger, 2013). The results, derived from a limited dataset, are depicted in rose diagrams (fig. 13C), displaying the mean paleocurrent values for the examined beds. These consistently reveal a westward to southwestward flow direction.

6. DISCUSSION

Based on the results presented in previous sections, we discuss the age, stratigraphy, correlations, and tectonic setting of the CMS and Trapa Trapa Formation. Integrating our findings with previous research conducted in the region, we propose a model for the tectono-stratigraphic evolution of the Andes of south-central Chile and Argentina during the late Cenozoic.

6.1. STRATIGRAPHY, AGE, AND CORRELATIONS

Debate persists over the stratigraphic framework and depositional ages of the Cenozoic units in the eastern Principal Cordillera of south-central Chile and Argentina (see previous section). Key issues include: 1) determining the age of the sedimentary rocks of the Cura Mallín Formation (CMS), 2) establishing the stratigraphic relationship between volcanic (CMV) and sedimentary (CMS) rocks attributed to this unit, 3) determining the age of the Trapa Trapa Formation, and 4) investigating correlations between the CMS and Trapa Trapa formations with Miocene deposits in the Agrio and Chos Malal FTBs, as well as other units within the Andes of south-central Chile and Argentina.

The primary issue concerning the age of the CMS arises from disparities in reported ages for this unit in Chile (Flynn et al., 2008; Suárez & Emparán, 1995, 1997) and Argentina (figs. 3, 4, and 5). In the Laguna del Laja area, Herriott (2006) and Flynn et al. (2008) obtained 14 Ar/Ar ages ranging from 19.8 to 14.5 Ma (early to middle Miocene) for the CMS (table 1). These ages partially coincide with our U-Pb ages for this unit in the same area. However, we obtained a younger maximum depositional age of <8.8 Ma for the upper part of the CMS, indicating an early-late Miocene range for this unit (fig. 7). These findings align with the K/Ar and U-Pb ages for the CMS in the Lonquimay area, which also indicate an early–late Miocene age (~20–11.6 Ma, table 1) (Encinas et al., 2022; Pedroza et al., 2017; Suárez & Emparán, 1995, 1997).

In contrast to these findings, Jordan et al. (2001) used the Ar/Ar method to date a pyroclastic interbed within the CMS in the Río Lileo area in Argentina, yielding an age of 22.8 Ma (fig. 3 and table 1). The sampled rock was situated in the upper part of the CMS, near the contact with the Trapa Trapa Formation (fig. 3). In our study, however, we obtained three U-Pb ages of <16.2, 13.6, and <12.5 Ma, from the upper part of this formation in the same area (fig. 3, and 7). These ages align with results from the Laguna del Laja and Lonquimay areas (Encinas et al., 2022; Flynn et al., 2008; Pedroza et al., 2017; Suárez & Emparán, 1995, 1997; and our study) and are also consistent with ages reported for Miocene sedimentary units in the Agrio and Chos Malal FTBs (table 1). The anomalously late Oligocene to early Miocene age reported by Jordan et al. (2001) for the

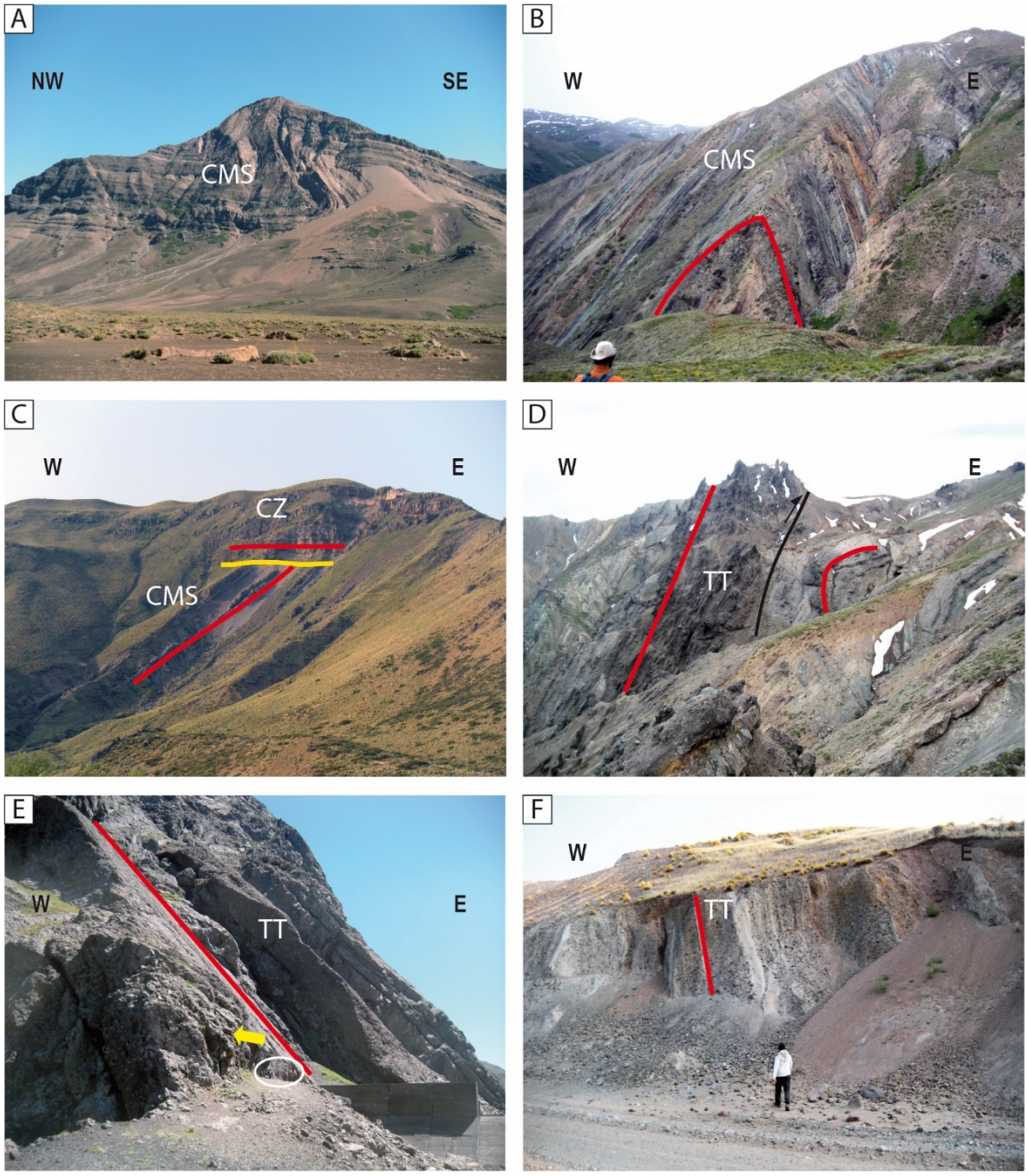

Figure 12. Evidence of post-depositional deformation in the CMS and Trapa Trapa formations (see fig. 3 for location details).

A) West-vergent Cerro Los Pinos anticline–syncline fold pair in the CMS, Laguna del Laja area. B) Tight chevron anticline in the CMS, Río Trapa-Trapa, Laguna del Laja area. C) Angular unconformity between the CMS and the Cola de Zorro Formation (CZ) in the Río Reñileuvú, Río Lileo area. D) West-vergent asymmetrical fold in the Trapa Trapa Formation (right side), Río Trapa-Trapa, Laguna del Laja area. Note subvertical strata in the western flank of the structure. A reverse fault to the west is inferred accommodating the tight deformation at the fold core. E) Steeply inclined (~50°E) strata of the Trapa Trapa Formation in the eastern limb of an anticline at the sky resort in the Laguna del Laja area (see also fig. 13). People are encircled for scale, and a yellow arrow points out to meter-sized clasts in boulder conglomerate. F) Subvertical (~80°E) conglomeratic strata of the Trapa Trapa Formation in the western limb of a syncline in the Río Reñileuvú, Río Lileo area.

upper part of the CMS may be an overestimation, possibly due to insufficient hornblende content in the sample (see fig. 5 in Jordan et al., 2001). Additionally, the absence of step heating in the analysis of this sample raises questions about the reliability of the results.

We believe that the new radiometric ages obtained in our study provide a resolution to the stratigraphic relationship between the CMV and CMS formations. Jordan et al. (2001) suggested that both units are coeval and laterally equivalent, based solely on two Ar/Ar ages: one for the basal part of the CMV (24.6 Ma) and one for the upper part of the CMS formation (22.8 Ma) in the Río Lileo area (fig. 3, and table 1). However, they did not observe direct interdigitation between these units. Our middle–late Miocene ages for the CMS formation in the same area support its correlation with sections of this unit in the Laguna del Laja area

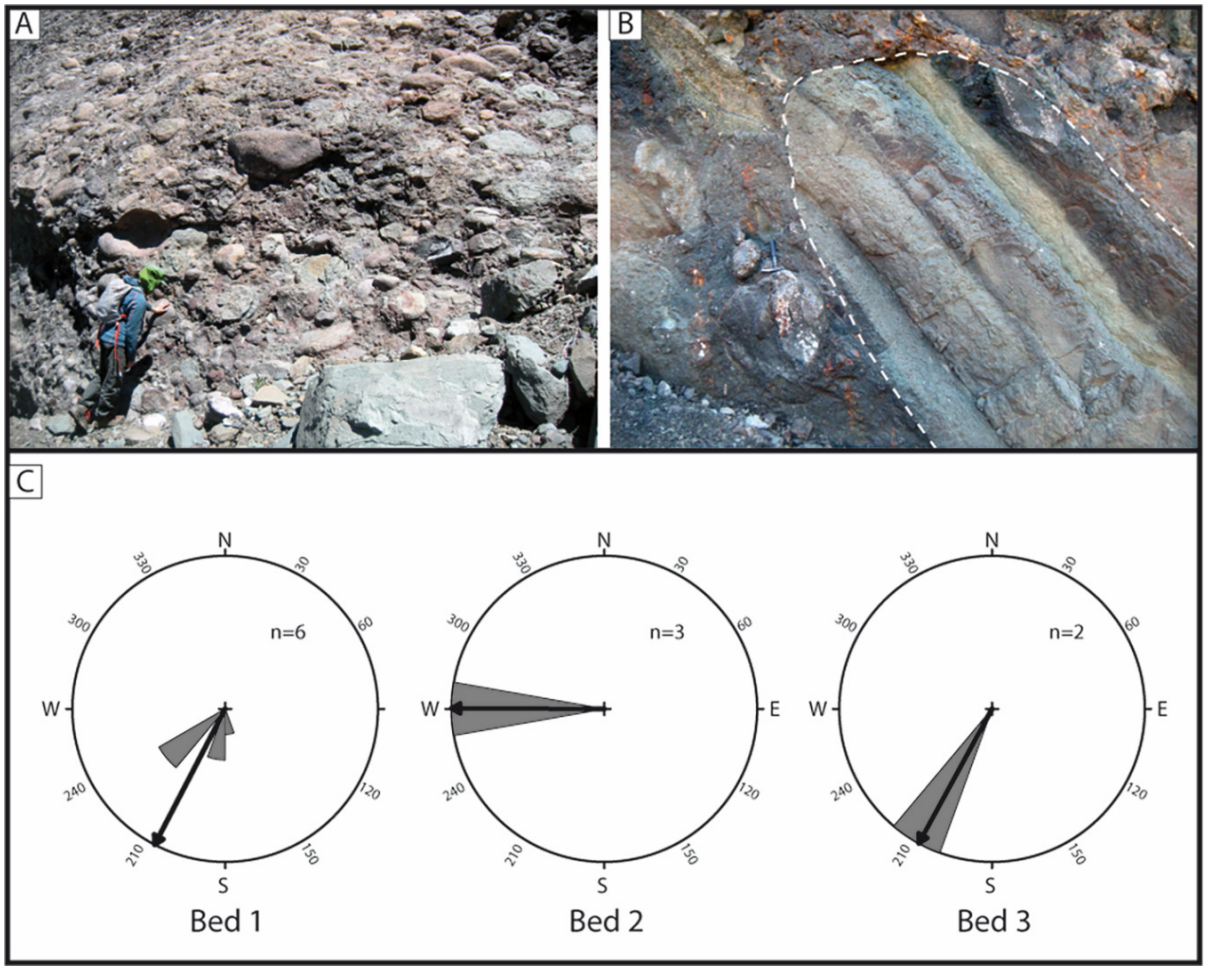

Figure 13. A) Boulder conglomerate with mostly subrounded clasts, ranging from decimeters to over 1 meter in diameter, in the Trapa Trapa Formation at the sky resort in the Laguna del Laja area (see figs. 3, and 12E). B) Subrounded imbricated megaclast (see hammer for scale) indicating a westward transport direction (Az 270° after bedding attitude restitution). C) Rose diagrams obtained with the Stereonet software for three different beds. Mean paleocurrents indicate W and SW transport directions.

to the west. Additionally, Utgé et al. (2009) and Espinach (2009) identified a clear contact relationship between the CMV and CMS formations in the Río Lileo area. Suárez and Emparán (1995, 1997) also correlated both units in the Lonquimay area (fig. 4) but suggested that the middle-late Miocene volcanic rocks in the western Principal Cordillera likely correspond to younger units. In fact, the oldest age for the CMV (22.0 Ma) reported by these authors (table 1) was obtained from a locality where Pedroza et al. (2017) and Encinas et al. (2022) observed a contact between this unit and the overlying CMS.

As for the age of the Trapa Trapa Formation, Flynn et al. (2008) reported two Ar/Ar ages of 10.1 and 8.9 Ma (late Miocene) for this unit in the Laguna del Laja area (fig. 3, and table 1). Burns et al. (2006) obtained similar Ar/Ar ages of approximately 11.7 and 10.8 Ma for the Trapa Trapa Formation in the Río Lileo area (fig. 3, and table 1). These ages align with the six K/Ar ages, ranging from 9.5 to 8.0 Ma, obtained for the equivalent Mitrauquén Formation in the Lonquimay area (table 1, Suárez & Emparán, 1995, 1997). In contrast, Jordan et al. (2001) reported a significantly older Ar/Ar age of 16.2 Ma for the Río Lileo area (fig. 3, and table 1). Our study yielded two U-Pb maximum depositional ages, <12.5 and <6.4 Ma, for the Trapa Trapa Formation in the Río Lileo area (figs. 3, and 7). The first age likely does not represent the true age of this unit, as it is similar to the age of <12.5 Ma for the CMS in the same area. While we did not obtain samples from the Laguna del Laja area, the age of <8.8 Ma for the upper part of the CMS, near the contact with the Trapa Trapa Formation (figs. 3, and 7), suggests a maximum age for the latter. In summary, these findings support a late Miocene age for the Trapa Trapa Formation.

6.2. TECTONIC SETTING FOR THE CURA MALLÍN FORMATION. EXTENSION VERSUS SHORTENING

The tectonic context during the deposition of the Cura Mallín Formation, which includes both volcanic (CMV) and sedimentary (CMS) units, has been a subject of extensive debate (fig. 4). Suárez and Emparán (1995, 1997) initially suggested local extension driven by the Liquiñe-Ofqui Fault Zone, although they lacked structural evidence. Jordan et

al. (2001) proposed that the Cura Mallín Formation accumulated in an intra-arc extensional basin based on their interpretation of the Repsol-YPFs seismic line 11128 in the Río Lileo area (see their fig. 7). They also indicated that tectonic inversion in the area likely occurred during or after the deposition of the Trapa Trapa Formation. Folguera et al. (2010) reprocessed the same seismic line and provided a similar explanation. However, Cobbold and Rossello (2003) and Cobbold et al. (2008) challenged Jordan et al.'s (2001) interpretation, citing the absence of normal faults younger than the Jurassic in outcrops from this region, the poor quality of the seismic line, and the lack of oil-well data to constrain subsurface stratigraphy. In fact, Espinach (2009) reinterpreted the same seismic line and identified east-vergent thrusts that align with field observations of significant contractional structures affecting Cenozoic units in the area. Building upon Jordan et al.'s (2001) interpretation, Radic et al. (2002) integrated stratigraphic data from the Principal Cordillera at 37°–39°S and suggested that the Cura Mallín Formation was deposited in two large diachronous half-graben sub-basins with opposite polarity, separated by an accommodation zone. However, due to the absence of a locality where a complete section of the Cura Mallín Formation is exposed, calculating reliable changes in stratigraphic thickness remains challenging.

Our structural and geochronologic data (see previous sections) indicate that most of the CMS was deposited within a contractional tectonic setting. Only the lower section of this unit seems to have been formed under extension, as evidenced by the presence of an inverted extensional wedge with an approximate age of ~20–19.5 Ma at the base of the Cerro Campamento section (figs. 3, and 8). Overlying these strata are syncontractional deposits dating to <18.7 Ma, marking the initiation of contractional deformation (figs. 3, 8, and 9). Further evidence of syncontractional sedimentation was observed in strata dating to <15.7 Ma at Baños Nitrao (figs. 3, 7, and 10) and in beds with ages ranging from <16.2 to 13.6 Ma at the Río Lileo (figs. 3, 7, and 11). Notably, the latter area aligns with where Cobbold and Rossello (2003) documented syncontractional growth strata. These findings are consistent with the results of Encinas et al. (2022), who also identified evidence of syntectonic sedimentation for the CMS in the Lonquimay area.

Structural data align with the findings from our provenance analysis. Given the current geological configuration and the prevailing river slopes in the Andes, which typically flow either eastward or westward, there are three potential sources of sediment for both the CMS and the Trapa Trapa Formation: the Coastal Cordillera, the western Principal Cordillera, and the Agrio and Chos Malal FTBs (as discussed in the previous section). Differentiating the provenance among these three areas is relatively straightforward due to the distinct ages of their rocks.

The Coastal Cordillera, located to the west of the CMS outcrops, is primarily composed of upper Paleozoic-Triassic metamorphic and plutonic rocks (fig. 2). However, this source is ruled out because there are no Miocene sedimentary deposits between this region and the CMS outcrops (Niemeyer & Muñoz, 1983; Sernageomin, 2003). In fact, the Central Depression is filled with Plio-Pleistocene deposits that unconformably overlie upper Oligocene-lower Miocene rocks (Encinas et al., 2021).

In the latitudes of our study area (37°–38°S), the western Principal Cordillera, situated immediately west of the CMS outcrops, comprises Oligo-Miocene volcanic and plutonic rocks, along with possible Upper Cretaceous plutonic rocks (figs. 2, and 3; Niemeyer & Muñoz, 1983; Spikings et al., 2008). In contrast, the Agrio and Chos Malal FTBs to the east consist of a wide variety of igneous and sedimentary rocks with ages spanning from Paleozoic, Permian, Triassic, Jurassic, Cretaceous, Paleocene, Eocene, Oligocene, to Miocene (Figs. 2, and 3; Rojas Vera et al., 2016). It is likely that sedimentary rocks in this region contain older recycled zircons.

All of the CMS detrital zircon samples we analyzed predominantly feature late Oligocene to Miocene groups (fig. 6, and table S1), strongly suggesting their origin from volcanic rocks of that age, primarily found in the western Principal Cordillera (fig. 2, and 3). This observation aligns with the presence of lower to middle Miocene nonmarine sedimentary rocks in the Agrio and Chos Malal FTBs, as well as in the foreland (figs. 2, and 3), indicating synchronous sedimentation to the east of the Principal Cordillera.

However, some of the CMS samples we analyzed also contain smaller groups of older zircons, which could suggest partial derivation from the Agrio and Chos Malal FTBs to the east (fig. 6). This implies that certain segments of this region may have undergone some degree of surface uplift due to earlier Late Cretaceous and Paleocene-Eocene deformation during CMS deposition, in line with proposals made by some authors (see Sánchez et al., 2018 and references therein). Another possibility is the contribution of recycled zircons from Oligocene-Miocene rocks in the western Principal Cordillera.

We did not observe any clear correlation between the age of the CMS analyzed samples and shifts in provenance. In the Cerro Campamento area (fig. 3), we examined two detrital zircon samples: CAMP-1 (<20.0 Ma) and ECZ-1 (<18.7 Ma). Only the latter contains a relatively larger proportion of Eocene, Mesozoic, and Paleozoic groups (fig. 6). However, this sample corresponds to a sandy tuff, and these zircons may have been incorporated from the bedrock through magmatic processes. Conversely, the younger samples BNIT-1 (<15.7 Ma) and BULD16-1 (<8.8 Ma), the latter positioned at the top of the CMS near the contact with the base of the Trapa Trapa Formation (fig. 3), exhibit only a few zircons of Cretaceous and Jurassic ages (fig. 6). Detrital zircon samples from the Río Lileo area in Argentina, close to the western boundary of the Agrio and Chos Malal FTBs (RL-1 and 17CMB-1), also predominantly display upper Oligocene to lower Miocene zircons, with fewer zircons of older ages, primarily Paleocene and Cretaceous (figs. 3, and 6). Our findings are in agreement with those of Encinas et al. (2022) in the Lonquimay area, who similarly proposed a western source for CMS sediment based on the predominance of Oligo-Miocene detrital zircons.

6.3. TECTONIC SETTING FOR THE TRAPA-TRAPA FORMATION. GROWTH OF THE AGRIO AND CHOS MALAL FTBS AND DEVELOPMENT OF A HINTERLAND BASIN

A significant shift in the tectono-sedimentary evolution of the eastern Principal Cordillera occurred around 9 Ma ago, coinciding with the cessation of CMS deposition and the initial accumulation of the Trapa Trapa Formation in the Laguna del Laja-Río Lileo area, along with its equivalent, the Mitrauquén Formation in the Lonquimay area. While the CMS primarily consists of sandstone, siltstone, and limited pebble or cobble conglomerates, occasionally intercalated with tuff layers, the Trapa Trapa and Mitrauquén Formations are characterized by predominantly cobble to boulder conglomerates (fig. 13), interspersed with andesites and ignimbrites.

This transition is accompanied by a distinct change in the source of sediment. Although detailed paleocurrent data are lacking, Encinas et al. (2022) reported eastward transport for the CMS in the Lonquimay area. This observation is corroborated by U-Pb geochronological data, which reveal a predominance of Oligo-Miocene detrital zircons, likely sourced from the western Principal Cordillera, in both the Laguna del Laja (fig. 6) and Lonquimay areas (Encinas et al., 2022). Furthermore, the presence of lower to middle Miocene strata in the Agrio and Chos Malal FTBs and the foreland indicates ongoing synorogenic nonmarine sedimentation to the east of the eastern Principal Cordillera (as discussed in the previous section).

Conversely, paleocurrents for imbricated clasts in the Trapa Trapa and Mitrauquén Formations, both in the Laguna del Laja (fig. 13) and Lonquimay areas, indicate a westward transport direction. However, the results from this study must be considered with caution, as they are based on limited measurements. Additionally, our sample 17MIT-1 exhibited a preponderance of Paleogene, Mesozoic, Paleozoic, and Precambrian U-Pb ages (fig. 6), clearly pointing to eastern sources in the Agrio and Chos Malal FTBs. Likewise, detrital zircons from the Mitrauquén Formation in the Lonquimay area exclusively exhibit Triassic, Paleozoic, and Precambrian ages, further supporting an eastern provenance (Encinas et al., 2022).

Furthermore, Melnick et al. (2006) identified the Pino Seco thrust as a west-vergent reverse fault that juxtaposed Jurassic marine strata over upper Miocene strata of the Mitrauquén Formation (fig. 2). The presence of growth strata at this site implies that the thrust was blind during the deposition of the Mitrauquén Formation, before it propagated to the surface (Encinas et al., 2022; Melnick et al., 2006). This structural and stratigraphic evidence is consistent with a westward propagation of deformation.

Our interpretations regarding the CMS and Trapa Trapa formations align with the Neogene tectono-sedimentary evolution of the Agrio and Chos Malal FTBs, as proposed by earlier researchers. These regions are predominantly characterized by Jurassic and Cretaceous rocks, with folded Oligo-Miocene strata typically confined to small outcrops within elevated synclines. This suggests that these formations experienced partial exhumation during regional deformation and rock uplift.

Radiometric data constrain the ages of thick successions of upper Oligocene to lower Miocene volcanic rocks, such as those of the Palaoco and Sierra Negra formations, which correlate with the CMV (table 1, Cobbold & Rossello, 2003; Garrido et al., 2012; Kay & Copeland, 2006; V. A. Ramos & Barbieri, 1989; Sagripanti et al., 2011, 2012; Silvestro & Atencio, 2009). These volcanic rocks are overlain by sedimentary and minor volcanic rocks primarily of early to middle Miocene age, determined mainly through the analysis of fossil mammals (table 1, Repol et al., 2002; Zamora Valcarce, 2007). These rocks have been interpreted as syncontractional deposits based on onlap relationships with older units, angular unconformities between different Miocene formations, growth strata, and provenance and paleocurrent analyses (Garrido et al., 2012; Sagripanti et al., 2011, 2012; Zamora Valcarce et al., 2006).

Geochemical data for Oligocene-Miocene volcanic rocks in this area suggest a transition from extension to contraction around 19 Ma ago (Kay & Copeland, 2006). Some middle Miocene units, such as the Tralalhue conglomerates, have been attributed to deposition in piggyback basins during the onset of deformation of the Agrio and Chos Malal FTBs (Garrido et al., 2012; V. A. Ramos, 1998; Zamora Valcarce, 2007; Zamora Valcarce et al., 2006). Folguera et al. (2007) proposed that shortening occurred in this area between approximately 15 and 12 Ma ago, based on structural relationships between deformed and undeformed rocks. Gürer et al. (2015) suggested that the emplacement of the Cerro Negro intrusive complex around 11.5 Ma ago was concurrent with shortening in the Chos Malal FTB. Sánchez et al. (2018) also recognized tectonically induced exhumation of this area at approximately 15–7 Ma ago, as determined through (U-Th)/He and fission track thermochronology. Lastly, Rodríguez et al. (2007) indicated that the upper Miocene to lower Pliocene El Palo Formation accumulated in the eastern foreland during peak deformation in the Agrio and Chos Malal FTBs.

While additional stratigraphic and geochronologic investigations are required to precisely constrain the tectonic evolution of the Agrio and Chos Malal FTBs, the existing data strongly suggest shortening during the late middle to early late Miocene. Thus, we propose that surface uplift of the Agrio and Chos Malal FTBs led to the division of the Miocene foreland basin that originally spanned from the eastern Principal Cordillera to the eastern craton. This division generated a topographically isolated hinterland basin within the eastern Principal Cordillera, where the Trapa Trapa Formation was deposited in an intermontane setting.

The deformation of the western flank of the Agrio and Chos Malal FTBs was primarily concentrated along the Andacollo and Loncopué Fault System (ALFS; Cobbold & Rossello, 2003), which delineates a distinct boundary with the Principal Cordillera to the west (figs. 2, 3). The oldest rock units in the study area, encompassing Paleozoic, Permian, and Triassic formations, are exposed immediately to the east of the ALFS within the Cordillera del Viento anticline (Cobbold & Rossello, 2003; Rojas Vera et al., 2016).

Sánchez et al. (2018) proposed that the ALFS was only active during the Late Cretaceous to early Paleogene. In contrast, Cobbold and Rossello (2003) suggested that it is a long-standing structural discontinuity that initially developed during the Permian and was subsequently reactivated during the Late Cretaceous to early Eocene, as well as during the Miocene to the present. Late Miocene reactivation is supported by fission-track data (Burns, 2002) and the deformation of middle to upper Miocene strata on both sides of the Cordillera del Viento (Folguera et al., 2007).

The presence of abundant detrital zircons with Triassic, Paleozoic, and Precambrian ages in samples from the Trapa Trapa Formation (fig. 6) and the Mitrauquén Formation (Encinas et al., 2022) strongly suggests the reactivation of the ALFS during the late Miocene. Detrital zircon samples from the CMS in the Río Lileo area (figs. 6, and 7, and table S1), near the Cordillera del Viento anticline, could further help pinpoint initial rock uplift within the range. While sample RL-1 (<16.2 Ma) in the Río Lileo area lacks zircons older than the Middle Jurassic, sample 17CMB-1 (<12.5 Ma) in the Reñileuvú river contains some zircons with Permo-Triassic and Paleozoic ages, possibly indicating the initiation of Neogene reactivation of the ALFS.

6.4. TECTONO-STRATIGRAPHIC EVOLUTION OF THE ANDES OF SOUTH-CENTRAL CHILE AND ARGENTINA DURING THE LATE CENOZOIC

Building on data collected in this study and information from prior research, we present our interpretation of the late Cenozoic tectono-stratigraphic evolution of the Andes in south-central Chile and Argentina (fig. 14).

During the Oligocene–early Miocene, extensional tectonics led to the development of a series of basins spanning the forearc, Andean Cordillera, and retroarc regions of southern South America between approximately 33° and 46° S (figs. 1, and 14A; Charrier et al., 2002; Encinas et al., 2016, 2018; Jordan et al., 2001; Kay & Copeland, 2006; Muñoz et al., 2000). The Cura Mallín Formation has traditionally been considered one of the volcano-sedimentary units deposited within these basins (Charrier et al., 2002; Jordan et al., 2001; Muñoz et al., 2000). Jordan et al. (2001) proposed that the lower volcanic (CMV) and upper sedimentary (CMS) units of the Cura Mallín Formation are coeval (fig. 4). They also suggested that the Cura Mallín Formation was deposited in an extensional intra-arc basin based on their interpretation of a seismic line in the Río Lileo area. Following Jordan et al.'s (2001) interpretation, subsequent studies by various authors have suggested that the Miocene deposits in the Agrio and Chos Malal FTBs were laid down after the inversion of the Cura Mallín basin (Folguera et al., 2007; Sagripanti et al., 2011, 2012; Zapata & Folguera, 2005).

Conversely, our data support the notion that the volcanic unit predates the sedimentary one, aligning with previous stratigraphic observations (Encinas et al., 2022; Espinach, 2009; Niemeyer & Muñoz, 1983; Pedroza et al., 2017; Utgé et al., 2009). According to the available data, the CMV is attributed to the Eocene–early Miocene (Contreras et al., 2022; Encinas et al., 2022; Jordan et al., 2001; Vergara et al., 1999) and can thus be correlated with the Abanico Formation and other units deposited in extensional basins along the margin. Our U-Pb data for the Laguna del Laja-Río Lileo areas indicate that the CMS was deposited during the early–late Miocene (figs. 3, 6, and 7, and table S1), consistent with previous studies in the Laguna del Laja and Lonquimay areas (table 1, Encinas et al., 2022; Flynn et al., 2008; Pedroza et al., 2017; Suárez & Emparán, 1995, 1997). Our geochronological and structural data also point to the transition from extensional to contractional deformation in the Laguna del Laja area occurring around 19 Ma during the initial CMS deposition (fig. 8). Provenance data indicate that the primary source area was situated in the western Principal Cordillera (fig. 6). Topographic growth in this area led to flexural subsidence and foreland sedimentation of the CMS and contemporaneous synorogenic deposits in the Agrio and Chos Malal FTBs, as well as the current foreland area to the east (fig. 14B). This notion is supported by the gradual thinning of these deposits, ranging from approximately 2000 to 2500 m in the eastern Principal Cordillera (Gutiérrez & Minniti, 1985; Herriott, 2006), around 400 m in the Agrio and Chos Malal FTBs, and about 200 m in the foreland (Rodríguez et al., 2007; Sagripanti et al., 2011, 2012) (fig. 14B).

Several studies have reported similar early Miocene ages for the onset of Andean uplift and foreland sedimentation in various locations along the Andes between ~33°–46°S (fig. 1; Cuitiño et al., 2016; Encinas et al., 2018; Folguera et al., 2018; Giambiagi et al., 2016; Horton & Fuentes, 2016; Rojas Vera et al., 2015). Consequently, the CMS can be correlated with the synorogenic deposits that accumulated during this phase, which extended across the eastern Andean Cordillera and the foreland. The scenario of the CMS resembles that of the Ñirihuau Formation. This non-marine succession, exposed around ~41°–43°S, exhibits similar facies to those found in the CMS and was initially thought to have been deposited in an extensional or transtensional setting during the late Oligocene–early Miocene (Jordan et al., 2001; Spalletti & Dalla Salda, 1996). However, subsequent studies presented structural, stratigraphic, and geochronological evidence indicating that at least a portion of this unit was deposited in a foreland basin during the early-middle to late Miocene (Bechis et al., 2014; Bechis & Cristallini, 2005; M. E. Ramos et al., 2011; Santonja et al., 2021).

The deposition of the upper part of the CMS during the middle to early late Miocene coincided with the progressive shortening of the Agrio and Chos Malal FTBs, resulting in sedimentation within local piggyback basins during this period (Garrido et al., 2012; V. A. Ramos, 1998; Zamora Valcarce, 2007; Zamora Valcarce et al., 2006). Around 9 Ma, the reactivation of the Andacollo and Loncopue Fault System (Cobbold & Rossello, 2003) led to focused uplift along the western flank of the Agrio and Chos Malal FTBs (fig. 14C). This event caused a significant shift in sedimentation within the eastern Principal Cordillera, marked by the accumulation of coarse-grained fluvial conglomerates found in the Trapa Trapa and Mitrauquén formations, originating from eastern sources as determined by provenance and pa-

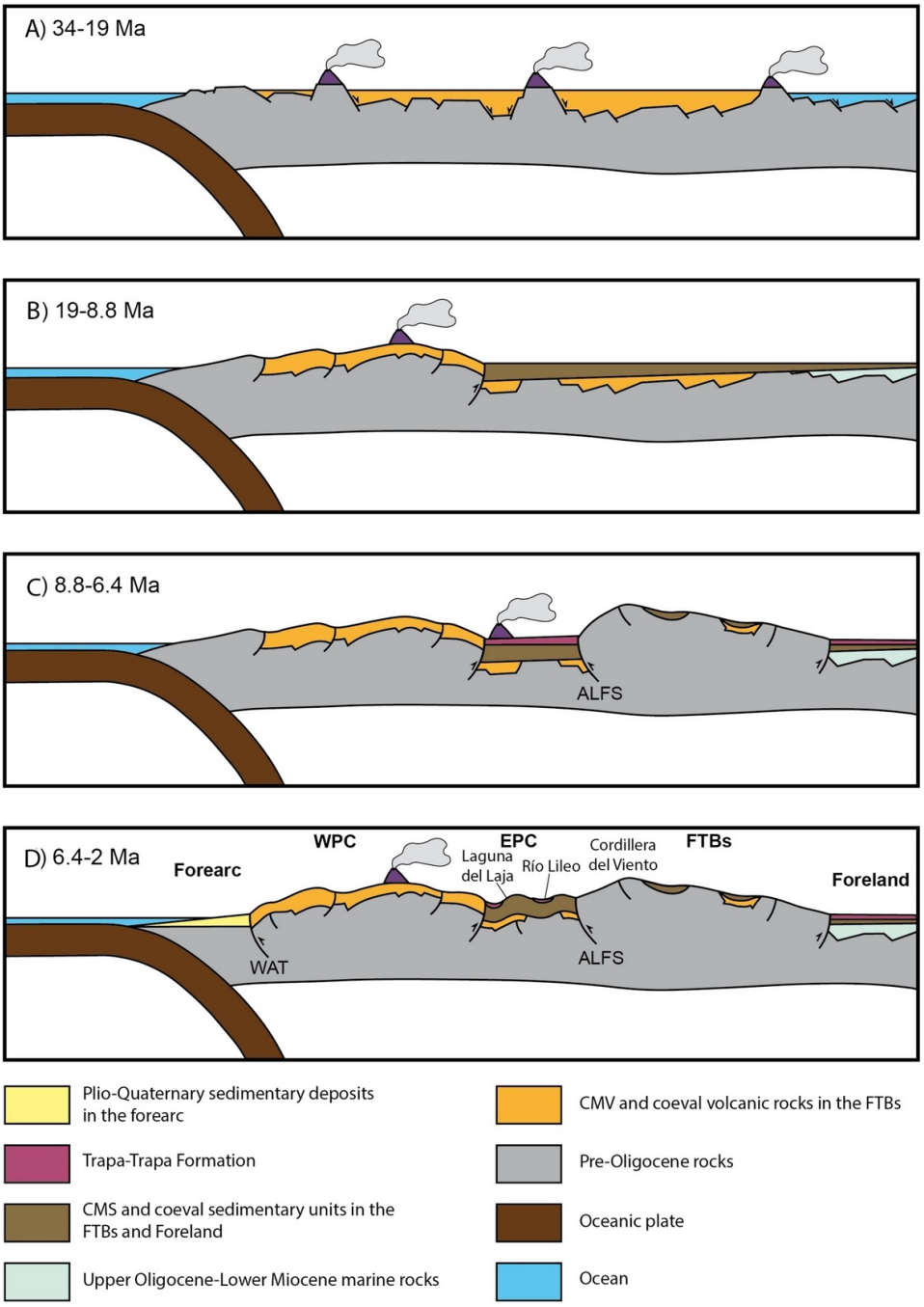

Figure 14. Schematic cross-sections, not to scale, illustrating the main phases of the inferred tectono-sedimentary evolution of the study area during the middle–late Cenozoic.

A) 34–19 Ma. Extensional tectonics led to regional subsidence and sedimentation of the CMV and the lower part of the CMS. Coeval volcanic units were deposited in the forearc to the west and the Agrio and Chos Malal Fold and Thrust Belts (FTBs) to the east. Marine strata were deposited in the foreland at the end of this interval. B) 19–.8 Ma. Shortening of the western Principal Cordillera (WPC) and deposition of the CMS and equivalent units in the FTBs and the foreland to the east. C) 8.8–6.4 Ma. Shortening of the FTBs led to the segmentation of the Miocene foreland basin and the development of a topographically isolated hinterland basin within the eastern Principal Cordillera. Deformation of the FTBs was primarily concentrated in the Andacollo and Loncopué Fault System (ALFS). Coarse-grained conglomerates and volcanic rocks of the Trapa Trapa Formation were deposited in the hinterland basin, between the western Principal Cordillera and the FTBs. Sediment of the Trapa Trapa Formation was derived from the Cordillera del Viento to the east as indicated by provenance and paleocurrent data. D) 6.4–2 Ma. Shortening migrated to the west causing major deformation of the CMS and the Trapa Trapa formations in the eastern Principal Cordillera first and then in rocks of the western Principal Cordillera. Shortening generated the West Andean Thrust (WAT) at the limit between the Principal Cordillera and the Central Depression. This triggered flexural subsidence and the accumulation of coarse-grained deposits in the forearc during the Pliocene–Pleistocene.

leocurrent analyses (see previous sections and Encinas et al., 2022).

After approximately 6.5 Ma (the youngest age for the Trapa Trapa Formation, figs. 6, and 7), deformation shifted westward, leading to intense folding of the lower to upper Miocene strata within the CMS, Trapa Trapa, and Mitrauquén formations (figs. 12, and 14d). It is likely that most of the west-vergent faults and folds affecting these units (Espinach, 2009; Melnick et al., 2006; Rojas Vera et al., 2016) were generated during this event. Notable examples include Cerro Los Pinos folds in Laguna del Laja (fig. 12A) and the Pino Seco thrust in the Lonquimay area (fig.

2; Encinas et al., 2022; Melnick et al., 2006). During this period, it is probable that the Principal Cordillera attained a higher elevation than during the preceding early-middle Miocene deformational phase, as suggested by paleontological studies (Solórzano et al., 2019). Deformation of the CMS, Trapa Trapa, and Mitrauquén formations in the eastern Principal Cordillera was relatively brief, as these units are unconformably overlain by nearly horizontal Plio-Pleistocene basalts of the Cola de Zorro Formation and equivalent units (figs. 8, 12C; Melnick et al., 2006; Muñoz & Niemeyer, 1984; Niemeyer & Muñoz, 1983; Rojas Vera et al., 2015; Suárez & Emparán, 1997), signaling the end of major deformation in this area. Nonetheless, some studies indicate the occurrence of minor folding and faulting affecting Plio-Pleistocene basaltic rocks and younger Quaternary sedimentary deposits in select locations within the eastern Principal Cordillera, the Agrio and Chos Malal FTBs, and the foreland, indicating more recent contractional deformation (Colavitto et al., 2019, 2020; Folguera et al., 2004, 2006; Galland et al., 2007; Messager et al., 2010; Sagripanti et al., 2015, 2018).

Recent studies indicate a significant Plio-Pleistocene uplift of the western Principal Cordillera in south-central Chile (Encinas et al., 2021). Deformation and surface uplift were concentrated along the West Andean Thrust, which marks the boundary between the western Principal Cordillera and the Central Depression (Armijo et al., 2010; Echaurren et al., 2022; Encinas et al., 2013; E. González, 1983; Melnick et al., 2006; Sepúlveda et al., 2019). This notion is supported by thermochronological data suggesting substantial late Miocene-Pliocene exhumation in the western Principal Cordillera (Adriasola et al., 2006; Glodny et al., 2008; Maksaev et al., 2009; Spikings et al., 2008; Thomson, 2002). Topographic loading led to flexural subsidence in the forearc, resulting in the accumulation of up to 2000 meters of Plio-Pleistocene conglomerates (Encinas et al., 2021) (fig. 14D).

An important implication of our studies relates to the kinematics and style of deformation in the Andes of central and south-central Chile and Argentina. Most studies have proposed that Neogene shortening of the Andean Cordillera in central and south-central Chile recorded continuous eastward propagation of retroarc deformation toward the foreland (Charrier et al., 2007; Farías et al., 2010; Giambiagi et al., 2003; Mpodozis & Ramos, 1990). In this framework, synorogenic strata in the foreland basin were progressively incorporated into the fold and thrust belt, which comprises east-vergent thrusts rooted in a major decollement with similar vergence (Astini & Dávila, 2010).

However, Armijo et al. (2010) (see also Rauld, 2011; Riesner et al., 2018) challenged this concept and proposed that deformation advanced westward toward the trench. Their argument was primarily based on predominant west-verging folds and thrusts affecting Oligo-Miocene volcanic rocks of the Abanico Formation along the western flank of the Principal Cordillera, as well as the presence of a major west-vergent fault (the West Andean Thrust) between this range and the Central Depression.

In contrast to the aforementioned models, our data suggest that the locus of shortening did not consistently advance eastward or westward. A summary of the sequence of events related to the deformational kinematics in the Andes of south-central Chile and Argentina is as follows (fig. 14B, C, D): 1) shortening initiated in the western Principal Cordillera during the early Miocene and propagated eastward; 2) the Agrio and Chos Malal FTBs experienced deformation during the middle to early late Miocene, resulting in the segmentation of the original foreland basin; 3) sedimentation persisted in the eastern Principal Cordillera, forming a hinterland basin, as well as in the contemporaneous foreland during the early late Miocene; 4) deformation became concentrated in the western region, leading to the folding and faulting of the CMS, Trapa Trapa, and Mitrauquén formations by the end of the late Miocene; 5) contractional deformation shifted farther westward, giving rise to the West Andean Thrust and Plio-Pleistocene uplift of the western flank of the Principal Cordillera. The suggested scenario indicates that the deformation in the study area initially propagated eastward during the early-middle Miocene and later shifted westward during the late Miocene-Pleistocene. Additional structural studies are needed to refine this model.

7. CONCLUSIONS

The Cura Mallín Formation has traditionally been considered an Oligocene-lower Miocene unit composed of coeval volcanic (CMV) and sedimentary (CMS) rocks deposited in an intra-arc basin during a regional phase of extensional tectonics. However, other studies proposed younger early–late Miocene ages for this unit and deposition of the CMS in a foreland basin. We conducted geochronological, structural, stratigraphic, and sedimentological studies to resolve these discrepancies. Based on our findings, we draw the following conclusions:

1. U-Pb ages from the Laguna del Laja-Río Lileo area indicate that the CMS was deposited during the early to late Miocene (~20–9 Ma), refuting the previous assignment of the upper part of this unit to the late Oligocene–early Miocene.
2. Structural data reveal that only the lower part of the CMS, dated at ~20 Ma, was deposited under extensional tectonics, while the rest of the unit, dated from ~19 to 9 Ma, was deposited under contractional conditions.
3. Provenance analysis based on U-Pb ages of detrital zircons suggests that the sediment source area for the CMS corresponds primarily to Oligocene-Miocene igneous rocks of the western Principal Cordillera.
4. Correlation of the CMS with synorogenic deposits in the Agrio and Chos Malal FTBs and the present foreland area suggests the existence of a lower-middle Miocene foreland basin that extended across these domains.
5. The CMS can be correlated with coeval lower-upper Miocene synorogenic units located along the eastern

part of the Andes and the foreland between ~33° and 46°S.

6. U-Pb ages from our study indicate that the volcano-sedimentary Trapa Trapa Formation was deposited during the late Miocene (~9–6.5 Ma), refuting the previous assignment of this unit to the late early Miocene.
7. Provenance data, derived from U-Pb dating of detrital zircons and paleocurrent analysis of clastic deposits of this unit, suggest a source area located in the western part of the Agrio and Chos Malal FTBs, to the east of the Principal Cordillera. Uplift of this range was mainly concentrated in the Andacollo and Loncopue Fault System, causing the segmentation of the foreland basin. The Trapa Trapa Formation was thus deposited in a topographically isolated hinterland basin.
8. After ~6.5 Ma, the locus of shortening shifted westward, resulting in intense folding of the CMS and Trapa Trapa Formation. The main deformation propagated westward during the Plio-Pleistocene, resulting in the thrusting of the western Principal Cordillera over the Central Depression and the deposition of synorogenic clastic deposits in the forearc.
9. These findings indicate that the locus of shortening during the Neogene growth of the Andes in this region did not consistently advance eastward or westward, challenging previous models. We suggest that the progression of deformation followed an initial eastward path during the early-middle Miocene and a westward path during the late Miocene to Pleistocene.

ACKNOWLEDGMENTS

AE was funded by ANID, Fondecyt project 1151146, and BH by the U.S. National Science Foundation grant EAR-1918541. We express our gratitude to Francisca Riffo and Hernán Arriagada for their assistance during fieldwork, and to Nicolás Orellana and Esteban Andrade for their contributions to the illustration of certain figures. We thank Mark Brandon, Michael Hren, Jon Spencer, and Chelsea Mackaman-Lofland for their detailed and constructive reviews, which significantly enhanced the previous version of the manuscript.

SUPPLEMENTARY DATA

https://doi.org/10.17632/kbyjyfxmty.1

Editor: Mark T. Brandon, Associate Editor: Michael Hren

Submitted: October 11, 2022 EDT, Accepted: February 25, 2024 EDT

REFERENCES

Adriasola, A. C., Thomson, S. N., Brix, M. R., Hervé, F., & Stöckhert, B. (2006). Postmagmatic cooling and late Cenozoic denudation of the North Patagonian Batholith in the Los Lagos region of Chile, 41°–42°15′S. *International Journal of Earth Sciences*, *95*(3), 504–528. https://doi.org/10.1007/s00531-005-0027-9

Allmendinger, R. W., Cardozo, N., & Fisher, D. M. (2011). *Structural Geology Algorithms*. Cambridge University Press. https://doi.org/10.1017/cbo9780511920202

Aragón, E., Castro, A., Díaz-Alvarado, J., & Liu, D.-Y. (2011). The North Patagonian batholith at Paso Puyehue (Argentina-Chile). SHRIMP ages and compositional features. *Journal of South American Earth Sciences*, *32*(4), 547–554. https://doi.org/10.1016/j.jsames.2011.02.005

Armijo, R., Rauld, R., Thiele, R., Vargas, G., Campos, J., Lacassin, R., & Kausel, E. (2010). The West Andean Thrust, the San Ramón Fault, and the seismic hazard for Santiago, Chile. *Tectonics*, *29*(2). https://doi.org/10.1029/2008tc002427

Astaburuaga, D. I. (2014). *Evolución estructural del límite mesozoico-cenozoico de la Cordillera principal entre 35°30' Y 36°S, Región del Maule, Chile: Tesis para optar al grado de Magíster en geología*. Universidad de Chile.

Astini, R. A., & Dávila, F. M. (2010). Comment on "The West Andean Thrust, the San Ramón Fault, and the seismic hazard for Santiago, Chile" by Rolando Armijo et al. *Tectonics*, *29*(4). https://doi.org/10.1029/2009tc002647

Barrio, C., Carlini, A. A., & Goin, F. J. (1986). Litogénesis y antigüedad de la Formación Chichinales de Paso Córdoba (Río Negro, Argentina. In *Congreso Argentino de Paleontología y Bioestratigrafía* (Vol. 4, pp. 149–156).

Bechis, F., & Cristallini, E. O. (2005). Tectonic evolution of northern Ñirihuau basin, northwestern Patagonia, Argentina. *6th International Symposium on Andean Geodynamics*, 103–106.

Bechis, F., Encinas, A., Concheyro, A., Litvak, V. D., Aguirre-Urreta, B., & Ramos, V. A. (2014). New age constraints for the Cenozoic marine transgressions of northwestern Patagonia, Argentina (41°–43° S): Paleogeographic and tectonic implications. *Journal of South American Earth Sciences*, *52*, 72–93. https://doi.org/10.1016/j.jsames.2014.02.003

Burns, W. M. (2002). *Tectonics of the Southern Andes from stratigraphic, thermochronologic, and geochemical perspectives* [Ph.D. thesis, Cornell University]. ProQuest Dissertations & Theses Global.

Burns, W. M., Jordan, T. E., Copeland, P., & Kelley, S. A. (2006). The case for extensional tectonics in the Oligocene-Miocene Southern Andes as recorded in the Cura Mallín basin (36°–38°S). *Evolution of an Andean Margin: A Tectonic and Magmatic View from the Andes to the Neuque´n Basin (35°-39°S Lat)*, 35–39. https://doi.org/10.1130/2006.2407(08)

Cardozo, N., & Allmendinger, R. W. (2013). Spherical projections with OSXStereonet. *Computers & Geosciences*, *51*, 193–205. https://doi.org/10.1016/j.cageo.2012.07.021

Carpinelli, A. A. (2000). *Análisis estratigráfico, paleoambiental, estructural y modelo tectono-estratigráfico de la cuenca de Cura-Mallín, VIII y IX región, Chile–Provincia del Neuquén, Argentina* [Undergraduate tesis]. Universidad de Concepción.

Cervera, M., & Leanza, H. A. (2009). Hallazgo de sedimentitas sinorogénicas neógenas en los alrededores de Chos Malal, Cuenca Neuquina, Argentina. *Revista Del Museo Argentino de Ciencias Naturales*, *11*(1), 15–22. https://doi.org/10.22179/revmacn.11.266

Chang, Z., Vervoort, J. D., McClelland, W. C., & Knaack, C. (2006). U-Pb dating of zircon by LA-ICP-MS. *Geochemistry, Geophysics, Geosystems*, *7*(5). https://doi.org/10.1029/2005gc001100

Charrier, R., Baeza, O., Elgueta, S., Flynn, J. J., Gans, P., Kay, S. M., Muñoz, N., Wyss, A. R., & Zurita, E. (2002). Evidence for Cenozoic extensional basin development and tectonic inversion south of the flat-slab segment, southern Central Andes, Chile (33°–36°S.L.). *Journal of South American Earth Sciences*, *15*(1), 117–139. https://doi.org/10.1016/s0895-9811(02)00009-3

Charrier, R., Pinto, L., & Rodríguez, M. P. (2007). Tectonostratigraphic evolution of the Andean Orogen in Chile. *The Geology of Chile*, 21–114. https://doi.org/10.1144/goch.3

Charrier, R., Wyss, A. R., Flynn, J. J., Swisher, C. C., III, Norell, M. A., Zapatta, F., McKenna, M. C., & Novacek, M. J. (1996). New evidence for late mesozoic-early Cenozoic evolution of the Chilean Andes in the upper Tinguiririca valley (35 °S), central Chile. *Journal of South American Earth Sciences*, *9*(5–6), 393–422. https://doi.org/10.1016/s0895-9811(96)00035-1

Cobbold, P. R., & Rossello, E. A. (2003). Aptian to recent compressional deformation, foothills of the Neuquén Basin, Argentina. *Marine and Petroleum Geology*, *20*(5), 429–443. https://doi.org/10.1016/s0264-8172(03)00077-1

Cobbold, P. R., Rossello, E. A., & Marques, F. O. (2008). Where is the evidence for Oligocene rifting in the Andes? Is it in the Loncopué Basin of Argentina? *7th International Symposium on Andean Geodynamics*.

Colavitto, B., Sagripanti, L., Fennell, L., Folguera, A., & Costa, C. (2019). Evidence of Quaternary tectonics along Río Grande valley, southern Malargüe fold and thrust belt, Mendoza, Argentina. *Geomorphology*, *346*, 106812. https://doi.org/10.1016/j.geomorph.2019.06.025

Colavitto, B., Sagripanti, L., Jagoe, L., Costa, C., & Folguera, A. (2020). Quaternary tectonics in the southern Central Andes (37°-38° S): Retroarc compression inferred from morphotectonics and numerical models. *Journal of South American Earth Sciences*, *102*, 102697. https://doi.org/10.1016/j.jsames.2020.102697

Colwyn, D. A., Brandon, M. T., Hren, M. T., Hourigan, J., Pacini, A., Cosgrove, M. G., Midzik, M., Garreaud, R. D., & Metzger, C. (2019). Growth and steady state of the Patagonian Andes. *American Journal of Science*, *319*(6), 431–472. https://doi.org/10.2475/06.2019.01

Contreras, J. P., Encinas, A., Muñoz-Gómez, M., Escribano, J., Castro, D., Vásquez, P., Folguera, A., Valencia, V., & Fanning, C. M. (2022). Nuevos antecedentes geocronológicos y estratigráficos de la localidad tipo de la Formación Colbún (Mioceno inferior), Región del Maule, Chile. *XXI Congreso Geológico Argentino, Puerto Madryn, Chubut*, 35–36.

Cuitiño, J. I., Fernicola, J. C., Kohn, M. J., Trayler, R., Naipauer, M., Bargo, M. S., Kay, R. F., & Vizcaíno, S. F. (2016). U-Pb geochronology of the Santa Cruz Formation (early Miocene) at the Río Bote and Río Santa Cruz (southernmost Patagonia, Argentina): Implications for the correlation of fossil vertebrate localities. *Journal of South American Earth Sciences*, *70*, 198–210. https://doi.org/10.1016/j.jsames.2016.05.007

Drake, R. E. (1976). Chronology of cenozoic igneous and tectonic events in the central Chilean Andes — latitudes 35° 30′ to 36°S. *Journal of Volcanology and Geothermal Research*, *1*(3), 265–284. https://doi.org/10.1016/0377-0273(76)90011-1

Echaurren, A., Encinas, A., Sagripanti, L., Gianni, G., Zambrano, P., Duhart, P., & Folguera, A. (2022). Fore- to-retroarc crustal structure of the north Patagonian margin: How is shortening distributed in Andean-type orogens? *Global and Planetary Change*, *209*, 103734. https://doi.org/10.1016/j.gloplacha.2022.103734

Elgueta, S., McDonough, M., Le Roux, J., Urqueta, E., & Duhart, P. (2000). Estratigrafía y sedimentología de las cuencas terciarias de la Región de Los Lagos (39–41°30'S). *Boletín de La Subdirección Nacional de Geología*, *57*, 1–50.

Encinas, A., Finger, K. L., Buatois, L. A., & Peterson, D. E. (2012). Major forearc subsidence and deep-marine Miocene sedimentation in the present Coastal Cordillera and Longitudinal Depression of south-central Chile (38 30'S-41 45'S). *Geological Society of America Bulletin*, *124*(7–8), 1262–1277. https://doi.org/10.1130/b30567.1

Encinas, A., Folguera, A., Bechis, F., Finger, K. L., Zambrano, P., Pérez, F., Bernabé, P., Tapia, F., Riffo, R., Buatois, L., Orts, D., Nielsen, S. N., Valencia, V. V., Cuitiño, J., Oliveros, V., De Girolamo Del Mauro, L., & Ramos, V. A. (2018). The Late Oligocene–Early Miocene Marine Transgression of Patagonia. *The Evolution of the Chilean-Argentinean Andes*, 443–474. https://doi.org/10.1007/978-3-319-67774-3_18

Encinas, A., Folguera, A., Oliveros, V., De Girolamo Del Mauro, L., Tapia, F., Riffo, R., Hervé, F., Finger, K. L., Valencia, V. A., Gianni, G., & Álvarez, O. (2016). Late Oligocene–early Miocene submarine volcanism and deep-marine sedimentation in an extensional basin of southern Chile: Implications for the tectonic development of the North Patagonian Andes. *Geological Society of America Bulletin*, *128*(5–6), 807–823. https://doi.org/10.1130/b31303.1

Encinas, A., Folguera, A., Riffo, R., Molina, P., Fernández Paz, L., Litvak, V. D., Colwyn, D. A., Valencia, V. A., & Carrasco, M. (2019). Cenozoic basin evolution of the Central Patagonian Andes: Evidence from geochronology, stratigraphy, and geochemistry. *Geoscience Frontiers*, *10*(3), 1139–1165. https://doi.org/10.1016/j.gsf.2018.07.004

Encinas, A., Pérez, F., Nielsen, S. N., Finger, K. L., Valencia, V., & Duhart, P. (2014). Geochronologic and paleontologic evidence for a Pacific–Atlantic connection during the late Oligocene–early Miocene in the Patagonian Andes (43–44°S). *Journal of South American Earth Sciences*, *55*, 1–18. https://doi.org/10.1016/j.jsames.2014.06.008

Encinas, A., Rosselot, E., Folguera, A., Orts, D., Sagripanti, L., Solórzano, A., Elesier, F., Opazo, E., & Valencia, V. (2022). Nuevos datos sedimentológicos y geocronológicos (U-Pb, LA-ICP-MS) para las rocas miocenas de la cuenca de Cura Mallín en el área de Lonquimay (38°-39°S). *XXI Congreso Geológico Argentino, Puerto Madryn, Chubut*, 1208–1209.

Encinas, A., Sagripanti, L., Rodríguez, M. P., Orts, D., Anavalón, A., Giroux, P., Otero, J., Echaurren, A., Zambrano, P., & Valencia, V. (2021). Tectonosedimentary evolution of the Coastal Cordillera and Central Depression of south-Central Chile (36°30′-42°S). *Earth-Science Reviews*, *213*, 103465. https://doi.org/10.1016/j.earscirev.2020.103465

Encinas, A., Zambrano, P. A., Finger, K. L., Valencia, V., Buatois, L. A., & Duhart, P. (2013). Implications of Deep-Marine Miocene Deposits on the Evolution of the North Patagonian Andes. *The Journal of Geology*, *121*(3), 215–238. https://doi.org/10.1086/669976

Espinach, S. (2009). *Geología de la zona de los altos de Buraleo (37°S, 71°O), Provincia de Neuquén* (p. 92) [Undergraduate Thesis]. Universidad de Buenos Aires.

Farías, M., Comte, D., Charrier, R., Martinod, J., David, C., Tassara, A., Tapia, F., & Fock, A. (2010). Crustal-scale structural architecture in central Chile based on seismicity and surface geology: Implications for Andean mountain building. *Tectonics*, *29*(3). https://doi.org/10.1029/2009tc002480

Fennell, L. M., Iannelli, S. B., Encinas, A., Naipauer, M., Valencia, V., & Folguera, A. (2019). Alternating contraction and extension in the Southern Central Andes (35°–37°S). *American Journal of Science*, *319*(5), 381–429. https://doi.org/10.2475/05.2019.02

Fernández Paz, L., Iannelli, S. B., Echaurren, A., Ramos, M., Bechis, F., Litvak, V. D., Encinas, A., Kasemann, S., Lucassen, F., & Folguera, A. (2020). The late Eocene–early Miocene El Maitén Belt evolution: Magmatic response to the changing subduction zone geodynamics. *Journal of South American Earth Sciences*, *103*, 102713. https://doi.org/10.1016/j.jsames.2020.102713

Flynn, J. J., Charrier, R., Croft, D. A., Gans, P. B., Herriott, T. M., Wertheim, J. A., & Wyss, A. R. (2008). Chronologic implications of new Miocene mammals from the Cura-Mallín and Trapa Trapa formations, Laguna del Laja area, south central Chile. *Journal of South American Earth Sciences*, *26*(4), 412–423. https://doi.org/10.1016/j.jsames.2008.05.006

Fock, A. (2005). *Cronología y tectónica de la exhumación en el Neógeno de los Andes de Chile Central entre los 33° y los 34°S* [Master thesis]. Universidad de Chile.

Fock, A., Charrier, R., Farías, M., & Muñoz, M. (2006). Fallas de vergencia oeste en la Cordillera Principal de Chile Central: Inversión de la cuenca de Abanico (33°-34°S). *Revista de La Asociación Geológica Argentina, Publicación Especial*, *6*, 48–55.

Folguera, A., Encinas, A., Echaurren, A., Gianni, G., Orts, D., Valencia, V., & Carrasco, G. (2018). Constraints on the Neogene growth of the central Patagonian Andes at the latitude of the Chile triple junction (45–47°S) using U/Pb geochronology in synorogenic strata. *Tectonophysics*, *744*, 134–154. https://doi.org/10.1016/j.tecto.2018.06.011

Folguera, A., Ramos, V. A., González Díaz, E. F., & Hermanns, R. (2006). Miocene to Quaternary deformation of the Guañacos fold-and-thrust belt in the Neuquén Andes between 37°S and 37°30′S. *Evolution of an Andean Margin: A Tectonic and Magmatic View from the Andes to the Neuque´n Basin (35°-39°S Lat)*. https://doi.org/10.1130/2006.2407(11)

Folguera, A., Ramos, V. A., Hermanns, R. L., & Naranjo, J. (2004). Neotectonics in the foothills of the southernmost central Andes (37°–38°S): Evidence of strike-slip displacement along the Antiñir-Copahue fault zone. *Tectonics*, *23*(5). https://doi.org/10.1029/2003tc001533

Folguera, A., Ramos, V. A., Zapata, T., & Spagnuolo, M. G. (2007). Andean evolution at the Guañacos and Chos Malal fold and thrust belts (36°30′–37°s). *Journal of Geodynamics*, *44*(3–5), 129–148. https://doi.org/10.1016/j.jog.2007.02.003

Folguera, A., Rojas Vera, E. A., Bottesi, G., Zamora Valcarce, G., & Ramos, V. A. (2010). The Loncopué Trough: A Cenozoic basin produced by extension in the southern Central Andes. *Journal of Geodynamics*, *49*(5), 287–295. https://doi.org/10.1016/j.jog.2010.01.009

Galland, O., Hallot, E., Cobbold, P. R., Ruffet, G., & de Bremond d'Ars, J. (2007). Volcanism in a compressional Andean setting: A structural and geochronological study of Tromen volcano (Neuquén province, Argentina). *Tectonics*, *26*(4). https://doi.org/10.1029/2006tc002011

García, F. (1968). Estratigrafía del Terciario de Chile central. In G. Cecioni (Ed.), *El Terciario de Chile Zona central* (pp. 25–57). Editorial Andrés Bello, Santiago de Chile.

García Morabito, E., & Ramos, V. A. (2012). Andean evolution of the Aluminé fold and thrust belt, Northern Patagonian Andes (38°30′–40°30′S). *Journal of South American Earth Sciences*, *38*, 13–30. https://doi.org/10.1016/j.jsames.2012.03.005

Garrido, A., Kramarz, A., Forasiepi, A., & Bond, M. (2012). Estratigrafía, mamíferos fósiles y edad de las secuencias volcanosedimentarias eoceno-miocenas de la sierra de Huantraico sierra Negra y cerro Villegas (provincia del Neuquén, Argentina). *Andean Geology*, *39*(3), 482–510. https://doi.org/10.5027/andgeov39n3-a07

Gehrels, G., Valencia, V., & Pullen, A. (2006). Detrital Zircon Geochronology by Laser-Ablation Multicollector ICPMS at the Arizona LaserChron Center. *The Paleontological Society Papers*, *12*, 67–76. https://doi.org/10.1017/s1089332600001352

Giambiagi, L. B., Mescua, J., Bechis, F., Hoke, G., Suriano, J., Spagnotto, S., Moreiras, S. M., Lossada, A., Mazzitelli, M., Dapoza, R. T., Folguera, A., Mardonez, D., & Pagano, D. S. (2016). Cenozoic Orogenic Evolution of the Southern Central Andes (32–36°S). *Springer Earth System Sciences*, 63–98. https://doi.org/10.1007/978-3-319-23060-3_4

Giambiagi, L. B., & Ramos, V. A. (2002). Structural evolution of the Andes in a transitional zone between flat and normal subduction (33°30′–33°45′S), Argentina and Chile. *Journal of South American Earth Sciences*, *15*(1), 101–116. https://doi.org/10.1016/s0895-9811(02)00008-1

Giambiagi, L. B., Ramos, V. A., Godoy, E., Alvarez, P. P., & Orts, S. (2003). Cenozoic deformation and tectonic style of the Andes, between 33° and 34° south latitude. *Tectonics*, *22*(4). https://doi.org/10.1029/2001tc001354

Glodny, J., Gräfe, K., Echtler, H., & Rosenau, M. (2008). Mesozoic to Quaternary continental margin dynamics in South-Central Chile (36–42°S): the apatite and zircon fission track perspective. *International Journal of Earth Sciences*, *97*(6), 1271–1291. https://doi.org/10.1007/s00531-007-0203-1

González, E. (1983). Geological and geophysical information for risk contracts. *Empresa Nacional Del Petróleo de Chile, Internal Report*.

González, O., & Vergara, M. (1962). *Reconocimiento geológico de la Cordillera de los Andes entre los paralelos 35° y 38°S*. Instituto de Geología, Universidad de Chile.

Gürer, D., Galland, O., Corfu, F., Leanza, H. A., & Sassier, C. (2015). Structure and evolution of volcanic plumbing systems in fold-and-thrust belts: A case study of the Cerro Negro de Tricao Malal, Neuquén Province, Argentina. *Geological Society of America Bulletin*, *128*(1–2), 315–331. https://doi.org/10.1130/b31341.1

Gutiérrez, A., & Minniti, S. (1985). *Comisión Geológica N° 1. Reconocimiento Geológico de las Nacientes del río Lileo, YPF report*. Departamento de Minas, Provincia del Neuquén.

Harland, W. B. (1977). International Stratigraphic Guide, 1976. *Geological Magazine*, *114*(3), 229–235. https://doi.org/10.1017/s0016756800044824

Herriott, T. M. (2006). *Stratigraphy, structure, and 40Ar/39Ar geochronology of the southeastern Laguna del Laja area: Implications for the mid-late Cenozoic evolution of the Andes near 37.5°S, Chile* [PhD Thesis]. University of California.

Hervé, F. (1994). The Southern Andes Between 39° and 44°S Latitude: The Geological Signature of a Transpressive Tectonic Regime Related to a Magmatic Arc. *Tectonics of the Southern Central Andes*, 243–248. https://doi.org/10.1007/978-3-642-77353-2_17

Horton, B. K. (2018). Tectonic Regimes of the Central and Southern Andes: Responses to Variations in Plate Coupling During Subduction. *Tectonics*, *37*(2), 402–429. https://doi.org/10.1002/2017tc004624

Horton, B. K., & Fuentes, F. (2016). Sedimentary record of plate coupling and decoupling during growth of the Andes. *Geology*, *44*(8), 647–650. https://doi.org/10.1130/g37918.1

Horton, B. K., Fuentes, F., Boll, A., Starck, D., Ramirez, S. G., & Stockli, D. F. (2016). Andean stratigraphic record of the transition from backarc extension to orogenic shortening: A case study from the northern Neuquén Basin, Argentina. *Journal of South American Earth Sciences*, *71*, 17–40. https://doi.org/10.1016/j.jsames.2016.06.003

Iannelli, S. B., Fennell, L. M., Litvak, V. D., Fernández Paz, L., Encinas, A., & Folguera, A. (2018). Geochemical and tectonic evolution of Late Cretaceous to early Paleocene magmatism along the Southern Central Andes (35-36°S). *Journal of South American Earth Sciences*, *87*, 139–156. https://doi.org/10.1016/j.jsames.2017.12.008

Jordan, T. E., Burns, W. M., Veiga, R., Pángaro, F., Copeland, P., Kelley, S., & Mpodozis, C. (2001). Extension and basin formation in the southern Andes caused by increased convergence rate: A mid-Cenozoic trigger for the Andes. *Tectonics*, *20*(3), 308–324. https://doi.org/10.1029/1999tc001181

Kay, S. M., & Copeland, P. (2006). Early to middle Miocene backarc magmas of the Neuquén Basin: Geochemical consequences of slab shallowing and the westward drift of South America. Evolution of an Andean Margin: A Tectonic and Magmatic View from the Andes to the Neuque´n Basin (35°-39°S lat). *Geological Society of America, Special Paper*, *407*. https://doi.org/10.1130/2006.2407(09)

Kellett, D. A., Cottle, J. M., & Larson, K. P. (2019). The South Tibetan Detachment System: history, advances, definition and future directions. *Geological Society, London, Special Publications*, *483*(1), 377–400. https://doi.org/10.1144/sp483.2

Lamb, S., & Davis, P. (2003). Cenozoic climate change as a possible cause for the rise of the Andes. *Nature*, *425*(6960), 792–797. https://doi.org/10.1038/nature02049

Leanza, H. A., Hugo, C. A., Repol, D., González, R., Danieli, J. C., & Lizuaín, A. (2001). Hoja Geológica 3969-I, Zapala, provincia del Neuquén. *Boletín Del Servicio Geológico Argentino, 275, Programa Nacional de Cartas Geológicas de La República Argentina, Scale 1:250.000*.

Lister, G., & Forster, M. (2009). Tectonic mode switches and the nature of orogenesis. *Lithos*, *113*(1–2), 274–291. https://doi.org/10.1016/j.lithos.2008.10.024

Ludwig, K. R. (2003). *Isoplot 3.0: A geochronological toolkit for Microsoft Excel* (p. 70). Berkeley Geochronology Center,.

Ludwig, K. R., & Mundil, R. (2002). Extracting reliable U-Pb ages and errors from complex populations of zircons from Phanerozoic tuffs. *Geochimica et Cosmochimica Acta*, *66, Supplement 1*, 463.

Maksaev, V., Munizaga, F., Zentilli, M., & Charrier, R. (2009). Fission track thermochronology of Neogene plutons in the Principal Andean Cordillera of central Chile (33-35°S): Implications for tectonic evolution and porphyry Cu-Mo mineralization. *Andean Geology*, *36*(2). https://doi.org/10.4067/s0718-71062009000200001

Martinod, J., Husson, L., Roperch, P., Guillaume, B., & Espurt, N. (2010). Horizontal subduction zones, convergence velocity and the building of the Andes. *Earth and Planetary Science Letters*, *299*(3–4), 299–309. https://doi.org/10.1016/j.epsl.2010.09.010

Melnick, D., & Echtler, H. P. (2006). Inversion of forearc basins in south-central Chile caused by rapid glacial age trench fill. *Geology*, *34*(9), 709–712. https://doi.org/10.1130/g22440.1

Melnick, D., Rosenau, M., Folguera, A., & Echtler, H. (2006). Neogene tectonic evolution of the Neuquén Andes western flank (37-39°S). Evolution of an Andean Margin: A Tectonic and Magmatic View from the Andes to the Neuque´n Basin (35°-39°S lat). *Geological Society of America, Special Papers*, *407*. https://doi.org/10.1130/2006.2407(04)

Messager, G., Nivière, B., Martinod, J., Lacan, P., & Xavier, J.-P. (2010). Geomorphic evidence for Plio-Quaternary compression in the Andean foothills of the southern Neuquén Basin, Argentina: NEUQUÉN ANDES COMPRESSION. *Tectonics*, *29*(4). https://doi.org/10.1029/2009tc002609

Mosolf, J. G., Gans, P. B., Wyss, A. R., Cottle, J. M., & Flynn, J. J. (2018). Late Cretaceous to Miocene volcanism, sedimentation, and upper-crustal faulting and folding in the Principal Cordillera, central Chile: Field and geochronological evidence for protracted arc volcanism and transpressive deformation. *GSA Bulletin*, *131*(1–2), 252–273. https://doi.org/10.1130/b31998.1

Mpodozis, C., & Ramos, V. (1990). The Andes of Chile and Argentina. In G. Ericksen, M. Cañas, & J. Reinemund (Eds.), *Geology of the Andes and its relation to hydrocarbon and mineral resources.* (Vol. 11, pp. 59–88). Circum-Pacific Council for Energy and Mineral Resources, Houston, Earth Science Series.

Muñoz, J. (1988). Volcanismo mioceno superior (Tortoniano) en la Región del Alto Biobío. *V Congreso Geológico Chileno*, *3*, 275–296.

Muñoz, J., & Niemeyer, H. (1984). *Hoja Laguna de Maule y del Biobío, Carta Geológica de Chile N°64*. Servicio Nacional de Geología y Minería, Santiago de Chile, Scale 1:250.000.

Muñoz, J., Troncoso, R., Duhart, P., Crignola, P., Farmer, L., & Stern, C. R. (2000). The relation of the mid-Tertiary coastal magmatic belt in south-central Chile to the late Oligocene increase in plate convergence rate. *Revista Geológica de Chile*, *27*(2). https://doi.org/10.4067/s0716-02082000000200003

Niemeyer, H., & Muñoz, J. (1983). *Hoja Laguna de La Laja: región de Bio Bio, Carta Geológica de Chile N°57*. Servicio Nacional de Geología y Minería, Santiago de Chile, Scale 1:250.000.

Oliveros, V., González, J., Espinoza Vargas, M., Vásquez, P., Rossel, P., Creixell, C., Sepúlveda, F., & Bastias, F. (2018). The Early Stages of the Magmatic Arc in the Southern Central Andes. *The Evolution of the Chilean-Argentinean Andes*, 165–190. https://doi.org/10.1007/978-3-319-67774-3_7

Oncken, O., Hindle, D., Kley, J., Elger, K., Victor, P., & Schemmann, K. (2006). Deformation of the Central Andean Upper Plate System — Facts, Fiction, and Constraints for Plateau Models. The Andes. *Frontiers in Earth Sciences. Springer, Berlin, Heidelberg*, 3–27. https://doi.org/10.1007/978-3-540-48684-8_1

Orts, D. L., Folguera, A., Encinas, A., Ramos, M., Tobal, J., & Ramos, V. A. (2012). Tectonic development of the North Patagonian Andes and their related Miocene foreland basin (41°30′-43°S). *Tectonics*, *31*(3). https://doi.org/10.1029/2011tc003084

Paces, J. B., & Miller, J. D., Jr. (1993). Precise U-Pb ages of Duluth Complex and related mafic intrusions, northeastern Minnesota: Geochronological insights to physical, petrogenetic, paleomagnetic, and tectonomagmatic processes associated with the 1.1 Ga Midcontinent Rift System. *Journal of Geophysical Research: Solid Earth*, *98*(B8), 13997–14013. https://doi.org/10.1029/93jb01159

Pascual, R., Bondesio, P., Vucetich, M. G., Scillato-Yané, G. J., Bond, M., & Tonni, E. P. (1984). Vertebrados fósiles cenozoicos. *X Congreso Geológico Argentino, San Carlos de Bariloche, Relatorio*, *II*(9), 439–461.

Paton, C., Woodhead, J. D., Hellstrom, J. C., Hergt, J. M., Greig, A., & Maas, R. (2010). Improved laser ablation U-Pb zircon geochronology through robust downhole fractionation correction. *Geochemistry, Geophysics, Geosystems*, *11*(3). https://doi.org/10.1029/2009gc002618

Pedroza, V., Le Roux, J. P., Gutiérrez, N. M., & Vicencio, V. E. (2017). Stratigraphy, sedimentology, and geothermal reservoir potential of the volcaniclastic Cura-Mallín succession at Lonquimay, Chile. *Journal of South American Earth Sciences*, *77*, 1–20. https://doi.org/10.1016/j.jsames.2017.04.011

Radic, J. P., Rojas, L., Carpinelli, A., & Zurita, E. (2002). Evolución Tectónica de la cuenca Terciaria de Cura-Mallín Región Cordillerana Chileno Argentina (36 30-39 00'S. *Congreso Geológico Argentino*, *15*, 233–237.

Ramos, M. E., Orts, D., Calatayud, F., Pazos, P. J., Folguera, A., & Ramos, V. A. (2011). Estructura, Estratigrafía y evolución tectónica de la cuenca de Ñirihuau en las nacientes del río Cushamen, Chubut. *Revista de La Asociación Geológica Argentina*, *68*(2), 210–224.

Ramos, V. A. (1998). Estructura del sector occidental de la faja plegada y corrida del Agrio, cuenca Neuquina, Argentina. *Congreso Latinoamericano de Geología, Buenos Aires*, *10*(2), 105–110.

Ramos, V. A., & Barbieri, M. (1989). El volcanismo Cenozoico de Huantraico: edad y relaciones isotópicas iniciales, provincia del Neuquén. *Revista de La Asociación Geológica Argentina*, *43*(2), 210–223.

Rauld, R. A. (2011). *Deformación cortical y peligro sísmico asociado a la falla San Ramón en el frente cordillerano de Santiago, Chile Central (33°S)* [Ph.D. tesis, Departamento de Geología, Universidad de Chile]. https://repositorio.uchile.cl/handle/2250/102600

Repol, D., Leanza, H. A., Sruoga, P., & Hugo, C. A. (2002). Evolución tectónica del Cenozoico de la comarca de Chorriaca, Provincia del Neuquén, Argentina. In *Congreso Geológico Argentino (El Calafate)* (Vol. 15).

Riesner, M., Lacassin, R., Simoes, M., Carrizo, D., & Armijo, R. (2018). Revisiting the crustal structure and kinematics of the Central Andes at 33.5°S: Implications for the mechanics of Andean mountain building. *Tectonics*, *37*(5), 1347–1375. https://doi.org/10.1002/2017TC004513

Rodríguez, M. F., Leanza, H. A., & Salvarredy Aranguren, M. (2007). Hoja Geológica 3969-II, Neuquén, provincias del Neuquén, Río Negro y La Pampa. *Programa Nacional de Cartas Geológicas de La República Argentina, Scale 1:250.000*, 370.

Rojas Vera, E. A., Mescua, J., Folguera, A., Becker, T. P., Sagripanti, L., Fennell, L., Orts, D., & Ramos, V. A. (2015). Evolution of the Chos Malal and Agrio fold and thrust belts, Andes of Neuquén: Insights from structural analysis and apatite fission track dating. *Journal of South American Earth Sciences*, *64*, 418–433. https://doi.org/10.1016/j.jsames.2015.10.001

Rojas Vera, E. A., Orts, D. L., Folguera, A., Zamora Valcarce, G., Bottesi, G., Fennell, L., Chiachiarelli, F., & Ramos, V. A. (2016). The Transitional Zone Between the Southern Central and Northern Patagonian Andes (36–39°S). In A. Folguera, M. Naipauer, L. Sagripanti, M. C. Ghiglione, D. L. Orts, & L. B. Giambiagi (Eds.), *Growth of the Southern Andes* (pp. 99–114). Springer Earth System Sciences. https://doi.org/10.1007/978-3-319-23060-3_5

Sagripanti, L., Bottesi, G., Kietzmann, D., Folguera, A., & Ramos, V. (2012). Mountain building processes at the orogenic front. A study of the unroofing in Neogene foreland sequence (37°S). *Andean Geology*, *39*(2), 201–219. https://doi.org/10.5027/andgeov39n2-a01

Sagripanti, L., Bottesi, G., Naipauer, M., Folguera, A., & Ramos, V. A. (2011). U/Pb ages on detrital zircons in the southern central Andes Neogene foreland (36°–37°S): Constraints on Andean exhumation. *Journal of South American Earth Sciences*, *32*(4), 555–566. https://doi.org/10.1016/j.jsames.2011.03.010

Sagripanti, L., Colavitto, B., Jagoe, L., Andrés, F., & Costa, C. (2018). A review about the quaternary upper-plate deformation in the Southern Central Andes (36–38°S): A plausible interaction between mantle dynamics and tectonics. *Journal of South American Earth Sciences*, *87*, 221–231. https://doi.org/10.1016/j.jsames.2017.11.008

Sagripanti, L., Folguera, A., Fennell, L., Rojas Vera, E. A., & Ramos, V. A. (2016). Progression of the Deformation in the Southern Central Andes (37°S). In A. Folguera, M. Naipauer, L. Sagripanti, M. C. Ghiglione, D. L. Orts, & L. B. Giambiagi (Eds.), *Growth of the Southern Andes* (pp. 115–132). Springer Earth System Sciences. https://doi.org/10.1007/978-3-319-23060-3_6

Sagripanti, L., Rojas Vera, E. A., Gianni, G. M., Folguera, A., Harvey, J. E., Farías, M., & Ramos, V. A. (2015). Neotectonic reactivation of the western section of the Malargüe fold and thrust belt (Tromen volcanic plateau, Southern Central Andes). *Geomorphology*, *232*, 164–181. https://doi.org/10.1016/j.geomorph.2014.12.022

Sánchez, N. P., Coutand, I., Turienzo, M., Lebinson, F., Araujo, V., & Dimieri, L. (2018). Tectonic Evolution of the Chos Malal Fold-and-Thrust Belt (Neuquén Basin, Argentina) From (U-Th)/He and Fission Track Thermochronometry. *Tectonics*, *37*(7), 1907–1929. https://doi.org/10.1029/2018tc004981

Santonja, C., Bechis, F., Suriano, J., Falco, J. I., Encinas, A., Olaizola, E. R., Valencia, V. A., Litvak, V. D., & Ramos, V. A. (2021). Tectono-stratigraphic evolution of the northeastern sector of the Ñirihuau basin, North Patagonian Andes, Argentina: Insights from sedimentology and geochronology data of the Ñirihuau Formation. *Journal of South American Earth Sciences*, *111*, 103487. https://doi.org/10.1016/j.jsames.2021.103487

Schlunegger, F., & Kissling, E. (2015). Slab rollback orogeny in the Alps and evolution of the Swiss Molasse basin. *Nature Communications*, *6*(1), 8605. https://doi.org/10.1038/ncomms9605

Schmitz, M. D., & Bowring, S. A. (2001). U-Pb zircon and titanite systematics of the Fish Canyon Tuff: an assessment of high-precision U-Pb geochronology and its application to young volcanic rocks. *Geochimica et Cosmochimica Acta*, *65*(15), 2571–2587. https://doi.org/10.1016/s0016-7037(01)00616-0

Sepúlveda, T., Cortés-Aranda, J., Melnick, D., Astudillo, L., Vega, A., & Poblete, C. (2019). Neotectónica y paleosismología del Cabalgamiento Andino Occidental (WATF) en la Región del Maule, Chile central (36°S). *Congreso Chileno de Sismología e Ingeniería Sísmica, Valdivia*, *12*, 1–15.

Sernageomin, S. (2003). *Mapa Geológico de Chile. Publicación Geológica Digital N°4 (CD-ROM, versión 1.0)*. Servicio Nacional de Geología y Minería, Santiago de Chile, Scale 1:1.000.000.

Silver, P. G., M. Russo, R., & Lithgow-Bertelloni, C. (1998). Coupling of South American and African Plate Motion and Plate Deformation. *Science*, *279*(5347), 60–63. https://doi.org/10.1126/science.279.5347.60

Silvestro, J., & Atencio, M. (2009). La cuenca cenozoica del río Grande y Palauco: edad, evolución y control estructural, faja plegada de Malargüe. *Revista de La Asociación Geológica Argentina*, *65*(1), 154–169.

Sláma, J., Košler, J., Condon, D. J., Crowley, J. L., Gerdes, A., Hanchar, J. M., Horstwood, M. S. A., Morris, G. A., Nasdala, L., Norberg, N., Schaltegger, U., Schoene, B., Tubrett, M. N., & Whitehouse, M. J. (2008). Plešovice zircon — A new natural reference material for U–Pb and Hf isotopic microanalysis. *Chemical Geology*, *249*(1–2), 1–35. https://doi.org/10.1016/j.chemgeo.2007.11.005

Solórzano, A., Encinas, A., Bobe, R., Maximiliano, R., & Carrasco, G. (2019). The Early to late Middle Miocene mammalian assemblages from the Cura-Mallín Formation, at Lonquimay, southern Central Andes, Chile (~38°S): Biogeographical and paleoenvironmental implications. *Journal of South American Earth Sciences*, *96*, 102319. https://doi.org/10.1016/j.jsames.2019.102319

Solórzano, A., Encinas, A., Kramarz, A., Carrasco, G., Montoya-Sanhueza, G., & Bobe, R. (2020). Late early Miocene caviomorph rodents from Laguna del Laja (~37° S), Cura-Mallín Formation, south-central Chile. *Journal of South American Earth Sciences*, *102*, 102658. https://doi.org/10.1016/j.jsames.2020.102658

Solórzano, A., Encinas, A., Kramarz, A., Carrasco, G., Montoya-Sanhueza, G., & Bobe, R. (2021). Late early Miocene mammals from Laguna del Laja, Cura-Mallín Formation, south-central Chile (~37°S) and their biogeographical and paleoenvironmental significance. *Journal of South American Earth Sciences*, *112*, 103544. https://doi.org/10.1016/j.jsames.2021.103544

Solórzano, A., Encinas, A., Kramarz, A., Carrasco, G., Núñez-Flores, M., & Bobe, R. (2023). A new pachyrukhine (Notoungulata: Typotheria) from the late Early Miocene of south-central Chile. *Historical Biology*, 1–15. https://doi.org/10.1080/08912963.2023.2214568

Somoza, R. (1998). Updated azca (Farallon)—South America relative motions during the last 40 My: implications for mountain building in the central Andean region. *Journal of South American Earth Sciences*, *11*(3), 211–215. https://doi.org/10.1016/s0895-9811(98)00012-1

Spalletti, L. A., & Dalla Salda, L. H. (1996). A pull apart volcanic related tertiary basin, an example from the Patagonian Andes. *Journal of South American Earth Sciences*, *9*(3–4), 197–206. https://doi.org/10.1016/0895-9811(96)00006-5

Spikings, R., Dungan, M., Foeken, J., Carter, A., Page, L., & Stuart, F. (2008). Tectonic response of the central Chilean margin (35–38°S) to the collision and subduction of heterogeneous oceanic crust: a thermochronological study. *Journal of the Geological Society*, *165*(5), 941–953. https://doi.org/10.1144/0016-76492007-115

Stern, R. J. (2002). Subduction zones. *Reviews of Geophysics*, *40*(4), 3–4. https://doi.org/10.1029/2001rg000108

Stinnesbeck, W. (1986). Zu den faunistischen und palokologischen Verhaltnissen in der Quiriquina Formation (Maastrichtium). *Zentrales-Chiles. Palaeontographica, Abteilung A*, *194*, 99–237.

Suárez, M., & Emparán, C. (1995). The stratigraphy, geochronology and paleophysiography of a Miocene fresh-water interarc basin, southern Chile. *Journal of South American Earth Sciences*, *8*(1), 17–31. https://doi.org/10.1016/0895-9811(94)00038-4

Suárez, M., & Emparán, C. (1997). *Hoja Curacautin: Regiónes de la Araucania y del Biobio, Regiones de la Araucanía y del Biobío, Carta Geológica de Chile N°71*. Servicio Nacional de Geología y Minería, Santiago, Chile, scale 1:250.000.

Thomson, S. N. (2002). Late Cenozoic geomorphic and tectonic evolution of the Patagonian Andes between latitudes 42°S and 46°S: An appraisal based on fission-track results from the transpressional intra-arc Liquiñe-Ofqui fault zone. *GSA Bulletin*, *114*(9), 1159–1173. https://doi.org/10.1130/0016-7606(2002)114<1159:lcgate>2.0.co;2

Utgé, S., Folguera, A., Litvak, V., & Ramos, V. A. (2009). Geología del sector norte de la Cuenca de Cura Mallín en las Lagunas de Epulaufquen, Neuquén. *Revista de La Asociación Geológica Argentina*, *64*(2), 231–248.

Uyeda, S., & Kanamori, H. (1979). Back-arc opening and the mode of subduction. *Journal of Geophysical Research: Solid Earth*, *84*(B3), 1049–1061. https://doi.org/10.1029/jb084ib03p01049

Valencia, V. A., Ruiz, J., Barra, F., Geherls, G., Ducea, M., Titley, S. R., & Ochoa-Landin, L. (2005). U–Pb zircon and Re–Os molybdenite geochronology from La Caridad porphyry copper deposit: insights for the duration of magmatism and mineralization in the Nacozari District, Sonora, Mexico. *Mineralium Deposita*, *40*(2), 175–191. https://doi.org/10.1007/s00126-005-0480-1

Vergara, M., Morata, D., Hickey-Vargas, R., López-Escobar, L., & Beccar, I. (1999). Cenozoic tholeiitic volcanism in the Colbún area, Linares Precordillera, central Chile (35°35'-36°S). *Revista Geológica de Chile*, *26*(1), 23–41. https://doi.org/10.4067/s0716-02081999000100002

Wells, M. L., Hoisch, T. D., Cruz-Uribe, A. M., & Vervoort, J. D. (2012). Geodynamics of synconvergent extension and tectonic mode switching: Constraints from the Sevier-Laramide orogen. *Tectonics*, *31*(1). https://doi.org/10.1029/2011tc002913

Williams, I. S. (1998). U-Th-Pb geochronology by ion microprobe. In M. A. McKibben, W. C. Shanks, & W. I. Ridley (Eds.), *Applications of microanalytical techniques to understanding mineralizing processes. Reviews in Economic Geology* (Vol. 7, pp. 1–35). Society of Economic Geologists.

Yáñez, G., & Cembrano, J. (2004). Role of viscous plate coupling in the late Tertiary Andean tectonics. *Journal of Geophysical Research: Solid Earth*, *109*(B2). https://doi.org/10.1029/2003jb002494

Zamora Valcarce, G. (2007). *Estructura y cinemática de la faja plegada del Agrio* [PhD tesis]. Universidad de Buenos Aires.

Zamora Valcarce, G., Zapata, T., Pino, D., & Ansa, A. (2006). Structural evolution and magmatic characteristics of the Agrio fold-and-thrust belt. In V. A. Ramos & S. M. Kay (Eds.), *Evolution of an Andean Margin: A Tectonic and Magmatic View from the Andes to the Neuque´n Basin (35°-39°S lat)* (Vol. 407, Issue 6, pp. 125–145). Geological Society of America.

Zanettini, J. C., Leanza, H. A., Giuisiano, A., & Santamaría, G. (2010). *Hoja Geológica 3972-II, Loncopué, provincia del Neuquén. Boletín del Servicio Geológico Minero Argentino 381*. Programa Nacional de Cartas Geológicas de La República Argentina, Scale 1:250.000.

Zapata, T., & Folguera, A. (2005). Tectonic evolution of the Andean Fold and Thrust Belt of the southern Neuquén Basin, Argentina. *Geological Society, London, Special Publications*, *252*(1), 37–56. https://doi.org/10.1144/gsl.sp.2005.252.01.03

SUPPLEMENTARY MATERIALS

Table S1

Download: https://ajsonline.org/article/115328-cenozoic-basin-evolution-during-alternating-extension-and-shortening-in-the-southern-central-andes-along-the-chile-argentina-border-37-38-s/attachment/220580.xlsx